· Article · Advances in Polar Science
doi: 10.12429/j.advps.2023.0036 March 2024 Vol. 35 No. 1: 78-107

A new look at the first dinosaur discovered in Antarctica: reappraisal of *Antarctopelta oliveroi* (Ankylosauria: Parankylosauria)

Sergio SOTO ACUÑA[1,2*], Alexander O. VARGAS[1] & Jonatan KALUZA[3,4]

[1] Red Paleontológica U-Chile, Departamento de Biología, Facultad de Ciencias, Universidad de Chile, Ñuñoa 7800003, Chile;
[2] Escuela de Geología, Facultad de Ciencias, Ingeniería y Tecnología, Universidad Mayor, Providencia, Santiago 7500994, Chile;
[3] Fundación de Historia Natural Félix de Azara, Universidad Maimónides, Buenos Aires C1405, Argentina;
[4] Consejo Nacional de Investigaciones Científicas y Técnicas (CONICET), Buenos Aires C1425FQB, Argentina

Received 31 December 2023; accepted 18 March 2024; published online 30 March 2024

Abstract The first dinosaur discovered in the Antarctic continent was the ankylosaur *Antarctopelta oliveroi* in the 1980s. Nevertheless, since then several hypotheses of phylogenetical relationships have been proposed because these have been depended on how the skeletal remains have been interpreted. The main obstacle for clarifying its phylogenetic position is that many portions of the skeleton remain unknown, in addition to the presence of unknown characters in typical ankylosaurs. Considered an ankylosaurid, nodosaurid, or even a chimaera, a recent proposal based on mostly complete material of a new ankylosaur from Chilean Patagonia provided support for a novel phylogenetic hypothesis: *Antarctopelta* and other southern ankylosaurs are an early branching clade, the Parankylosauria, whose origin probably dates to the Late Jurassic. In the light of this new view, a redescription of the available skeletal remains is provided together with a new reconstruction of the first Antarctic dinosaur known to the science community.

Keywords **Antarctic Peninsula, Biogeographic Weddellian Province, Parankylosauria, *Antarctopelta***

Citation: Soto Acuña S, Vargas A O, Kaluza J. A new look at the first dinosaur discovered in Antarctica: reappraisal of *Antarctopelta oliveroi* (Ankylosauria: Parankylosauria). Adv Polar Sci, 2024, 35(1): 78-107, doi: 10.12429/j.advps.2023.0036

1 Introduction

The Ankylosauria (Dinosauria: Ornithischia) were a successful clade that spanned at least from the Callovian to the Maastrichtian (Arbour and Mallon, 2017; Carpenter, 2004; Lydekker, 1893) and their remains have been discovered in all continents (Arbour and Currie, 2016). However, there is an asymmetry in the knowledge of Laurasian ankylosaur vs. Gondwanan ankylosaurs (Pereda-Suberbiola et al., 2015), which could be related to the reduced presence of available continental rocks along with the anthropogenic factor of fewer systematic paleontological prospections in Southern Hemisphere continents (Maidment et al., 2020).

Traditionally ankylosaurs have been divided in two clades (Coomb and Maryanska, 1990; Vickaryous et al., 2004): (1) the Nodosauridae, "lightly armored", except for the presence of big cervical and scapular spikes (typically greater than the antero-posterior length of the dorsal centers), elongated skulls (longer than wider) and possessors of a sacral shield armor that cover the entire

* Corresponding author, ORCID: 0000-0002-9311-9355, E-mail: sesotacu@ug.uchile.cl

pelvis (Coombs, 1978; Sereno, 1986); and (2) the Ankylosauridae, robust and heavily armored, with shorter than wider skulls, and with a tail-club weaponry (Coombs, 1978; Maryanska, 1977; Sereno, 1986). Nodosaurs are sometimes divided into more groups, one of them so called the "polacanthids" (Carpenter, 2001) and there is little consensus about their monophyly (Arbour et al., 2016; Thompson et al., 2012). Nodosaurid fossil record is well-known in the Jurassic and Cretaceous of North America (Carpenter et al., 1998; Eaton, 1960; Kirkland and Carpenter, 1994; Lambe, 1919; Ostrom, 1970; Parks, 1924), Europe (Bunzel, 1871; Galton, 1980; Kirkland et al., 2013; Mantell, 1833; Nopcsa, 1915; Ősi, 2005) and less known in Asia (Yang et al., 2013). Furthermore, ankylosaurids *sensu stricto* appear in the fossil record during the "mid" Cretaceous (Tumanova, 1983; Xu et al., 2001; Zheng et al., 2018), and they have been recovered from North America (Arbour and Currie, 2013a; Brown, 1908; Lambe, 1902; Nopcsa, 1928; Penkalski, 2001, 2013, 2018) and Asia (Arbour and Currie, 2013b; Gilmore, 1930; Han et al., 2014; Maleev, 1955; Maryanska, 1977; Xu et al., 2001). There is no reliable record of Ankylosauridae in Europe, with the possible exception of *Hylaeosaurus*, which could be an early-diverging ankylosaurid (Arbour et al., 2016; Zheng et al., 2018), but still has a highly unstable phylogenetic position in recent analyses (Raven et al., 2023; Soto-Acuña et al., 2021).

Otherwise, the Gondwanan fossil record of ankylosaurs has been scarce and discontinuous during the Mesozoic (Maidment et al., 2021; Pereda-Suberbiola et al., 2015; Rozadilla et al., 2021). Besides isolated (Galton, 2019) or unconfirmed reports of ankylosaurs in India (Chatterjee and Rudra, 1996) and Madagascar (Piveteau, 1926), the most relevant and informative record comes from the Eromanga-Surat Basin, in Eastern Australia. This includes *Minmi paravertebra* (specimen F10329), from the lower Aptian Bungil Formation (Molnar, 1980), *Kunbarrasaurus ieversi* (specimen QM F18101) from the Albian–Cenomanian Allaru Mudstone (Molnar, 1996) and cf. *Kunbarrasaurus* (specimen SAMA P40536) from the Albian Toolebuc Formation (Frauenfelder et al., 2022) in Queensland, Australia. A third unnamed taxon from this last formation has been also preliminarily reported (Leahey et al., 2019). Several other Australian isolated records include ankylosaur teeth from the Albian-Turonian Winton Formation (Leahey and Salisbury, 2013); osteoderms from the Turonian Griman Creek Formation (Bell et al., 2018); and teeth and vertebral elements from both the Barremian-Aptian "Wonthaggi" Formation and the Aptian-Albian Eumeralla Formation, in Victoria, South Australia (Barrett et al., 2010; Poropat et al., 2018). In summary, the fossil record of ankylosaurs in Australia is relatively continuous between the Barremian–Turonian stages. On the other hand, fragmentary remains of caudal vertebrae and ribs referable to indeterminate ankylosaurs were reported from the Campanian Tahora Formation, in New Zealand (Molnar and Wiffen, 1994).

The Antarctic record is mainly represented by *Antarctopelta oliveroi*, whose holotype MLP-PV 86-X-28-1 and the only known specimen was discovered by both participants in the field work organized by the Instituto Antártico Argentino carried out in the summer of 1986 (Gasparini et al., 1987; Olivero et al., 1991). Most recently, Coria et al. (2011) relocated the *Antarctopelta* discovery site and collected additional elements, presumably from the same specimen. The material, assumed to represent one individual, was initially described by Gasparini et al. (1987) and referred to the family Ankylosauridae. Posteriorly an expanded description by Olivero et al. (1991), brought more stratigraphical detail and discussed the palaeobiogeographical implications of the discovery for first time. Two hypotheses are mentioned: (1) an early divergence of ankylosaurids in Antarctica during the Jurassic or (2) an incursion of North American ankylosaurids during the late Cretaceous to South America and then Antarctica, and the second one is preferred hypothesis (Olivero et al., 1991). A few years later a new description of the specimen is made by Gasparini et al. (1996), where a re-assignation to the family Nodosauridae is proposed, argued on the morphology of the teeth. This idea was also consistent with the supposed presence of nodosaurs in the Argentine Patagonia (Salgado and Coria, 1996), supporting the hypothesis of a dispersion event from North America to South America. Finally, a more detailed description was presented in, with a new name for the specimen, *Antarctopelta oliveroi* (Salgado and Gasparini, 2006), reaffirming its affinities with Nodosauridae. At the time, the cladistic analysis of Ankylosauria was in its beginnings (Carpenter, 2001; Carpenter et al., 1998; Lee, 1996). The first inclusion of *A. oliveroi* in a matrix was made by Thompson et al. (2012), where an early-diverging position was recovered for the taxon. Arbour and Currie (2016) subsequently found *A. oliveroi* in a slightly more "derived" position within Nodosauridae, although they invalidated the taxon under the argument that the holotype was a chimera of different taxa. Distal and mid caudal vertebrae of *Antarctopelta* were interpreted by them as belonging to elasmosaurs and mosasaurs respectively. However, neither the distal and the caudal vertebra have synapomorphies of Elasmosauridae and Mosasauridae, and the presence of ossified tendons in the distal caudal vertebra allowed to discard their assignment to marine reptiles (Rozadilla et al., 2021). However, a strange combination of characteristics, including pieces of highly vascularized and ornamented flat osteoderms larger than any vertebra, together with posterior caudals highly depressed in dorso-ventral direction and the unique morphology of supposed cranial bones made *Antarctopelta* a very strange ankylosaur of uncertain affinities.

The discovery of a virtually complete skeleton of a new ankylosaur in Subantarctic Chilean Patagonia, *Stegouros elengassen*, from the Campanian–Maastrichtian Dorotea Formation, allowed to reinterpret many of the

bizarre traits of *Antarctopelta oliveroi*, which also seems to be present in other Gondwanan ankylosaurs (Soto-Acuña et al., 2021). Moreover, recent discoveries of new South American armored dinosaurs, including *Patagopelta cristata* from the Campanian–Maastrichtian Allen Formation from Argentine Patagonia (Riguetti et al., 2022), and other records under study confirms the existence of an early splitting lineage of ankylosaurs, the Parankylosauria (Agnolin et al., 2023; Becerra et al., 2023; Frauenfelder et al., 2022; Pol et al., 2023; Soto-Acuña et al., 2021). The relatedness with other Australian ankylosaurs also lends strong support for a paleobiogeographical connection of Weddellian parankylosaurs, with probable incursion of them from Australia to Patagonia via Antarctica. In this work, a more detailed description and re-interpretation of the skeletal elements of *Antarctopelta oliveroi* is provided, in addition to further discussion of its palebiogeographical implications.

2 Stratigraphic and geographical frameworks

The James Ross Basin contains one of the most complete upper Cretaceous–Eocene sedimentary records in the Southern Hemisphere, spanning from the Barremian stage to the upper Eocene (Crame et al., 1991; Milanese et al., 2017, 2019, 2020; Olivero, 2012a; Witts et al., 2016). Considered a sub-basin of the Larsen Basin (del Valle et al., 1992; Macdonald et al., 1988), its sediments are currently exposed in the Northwestern zone of the Antarctic Peninsula. At the same time, the James Ross Basin (or sub-Basin) was in close contact with the Magallanes (Austral) Basin in South Patagonia at the end of the Cretaceous (Jordan et al., 2020; Reguero and Goin, 2021).

Within the lithostratigraphic units preserved in this basin, one of the most interesting for vertebrate paleontologists is the Marambio Group, due to the presence of late Cretaceous dinosaurs (Lamanna et al., 2019; Reguero et al., 2013). This group crops in several islands including James Ross Island, Vega Island, Snow Hill Island, Seymour (Marambio) Island, Cockburn Island, among others (Crame et al., 1991). Currently the Marambio Group is subdivided in the following formations, from older to younger: Santa Marta Formation of Santonian–Campanian age; Snow Hills Island of Campanian to Maastrichtian age; and López de Bertodano Formation of Maastrichtian–Danian age (Milanese et al., 2020; Roberts et al., 2014). Finally, the Snow Hills Island is subdivided in the Units A, B and C; being equivalent to the Gamma Formation (late Campanian) previously referred to Santa Marta Formation (Figures 1a–1c). From this last unit MLP-PV 86-X-28-1 were recovered (Figures 1a–1c). Also, from near levels the ornithopod *Trinisaura santamartensis* (MLP-PV 08-III-1-1) and an indeterminate titanosaur (MLP-PV 11-II-20-1) and several other marine vertebrates were recovered (Cerda et al., 2012; Coria et al., 2013; Reguero et al., 2022).

The Gamma Member consist of 280 m of fine-medium grained silty sandstones, with glauconite and carbonaceous mudstones with lens of pebbly sandstone to medium conglomerates (Olivero et al., 1991). The fossil-bearing level of MLP-PV 86-X-28-1 is located in the lower section of the Gamma Member, where the predominant lithology consists in bioturbated silty sandstone intercalated with carbonaceous mudstones (Olivero et al., 1991). Fossil traces are present in the most of the silty sandstone, including the ichnogenera *Thalassinoides*, *Skolithos* and *Ophiomorpha* (Olivero et al., 1991). Isolated teeth of elasmobranchians like *Notidanodon* were founded in direct association with the skeleton (Figure 1e) as well as bony fishes and nautiloids (Olivero et al., 1991).

The integration of data from ammonite and palynomorph biostratigraphy (Barreda et al., 1999; Kennedy et al., 2007; Olivero, 2012b) as well as $^{87}Sr/^{86}Sr$ chemostratigraphy (Crame et al., 2006; McArthur et al., 2000) and magnetostratigraphy (Milanese et al., 2020), allows to constrain the fossil bearing level to the Upper Campanian.

3 Material and methods

3.1 Collection and preparation

MLP-PV 86-X-28-1 was collected during the Instituto Antártico Argentino fieldwork carried out in 1986, associated with marine reptiles and elasmobranchians. Currently most of the specimen is housed in the Vertebrate Paleontology Collection of the Museo de La Plata. Some parts of the specimen were re-prepared by one of the present authors (Jonatan Kaluza) in recent years.

3.2 Phylogenetic analysis

To test the phylogenetic relationships of *Antarctopelta oliveroi*, a parsimony analysis was performed in TNT 1.5 (Goloboff and Catalano, 2016). The selected character matrix was one of those published in Soto-Acuña et al. (2021), which in turn is a modification of the original matrix of Arbour and Currie (2016). The matrix (191×67) was constructed and modified in Mesquite (Maddison and Maddison, 2019). Modifications to this matrix include 30 changes in the coding of *Hylaeosaurus* (Raven et al., 2020), 6 changes in *Patagopelta* and 5 in *Antarctopelta*, based on direct review of the specimens. Added to the above is the incorporation of 2 taxa, *Minmi paravertebra* and cf. *Kunbarrasaurus* SAMA P40536. Two characters taken from Frauenfelder et al. (2022) and Riguetti et al. (2022) matrices, respectively, were added (Supplementary Text S1 and Matrix S1).

For the search for the most parsimonious trees (MPTs), the analysis was conducted by a heuristic search on Wagner trees using tree bisection–reconnection. Random addition sequences were performed holding 10 trees per replicate.

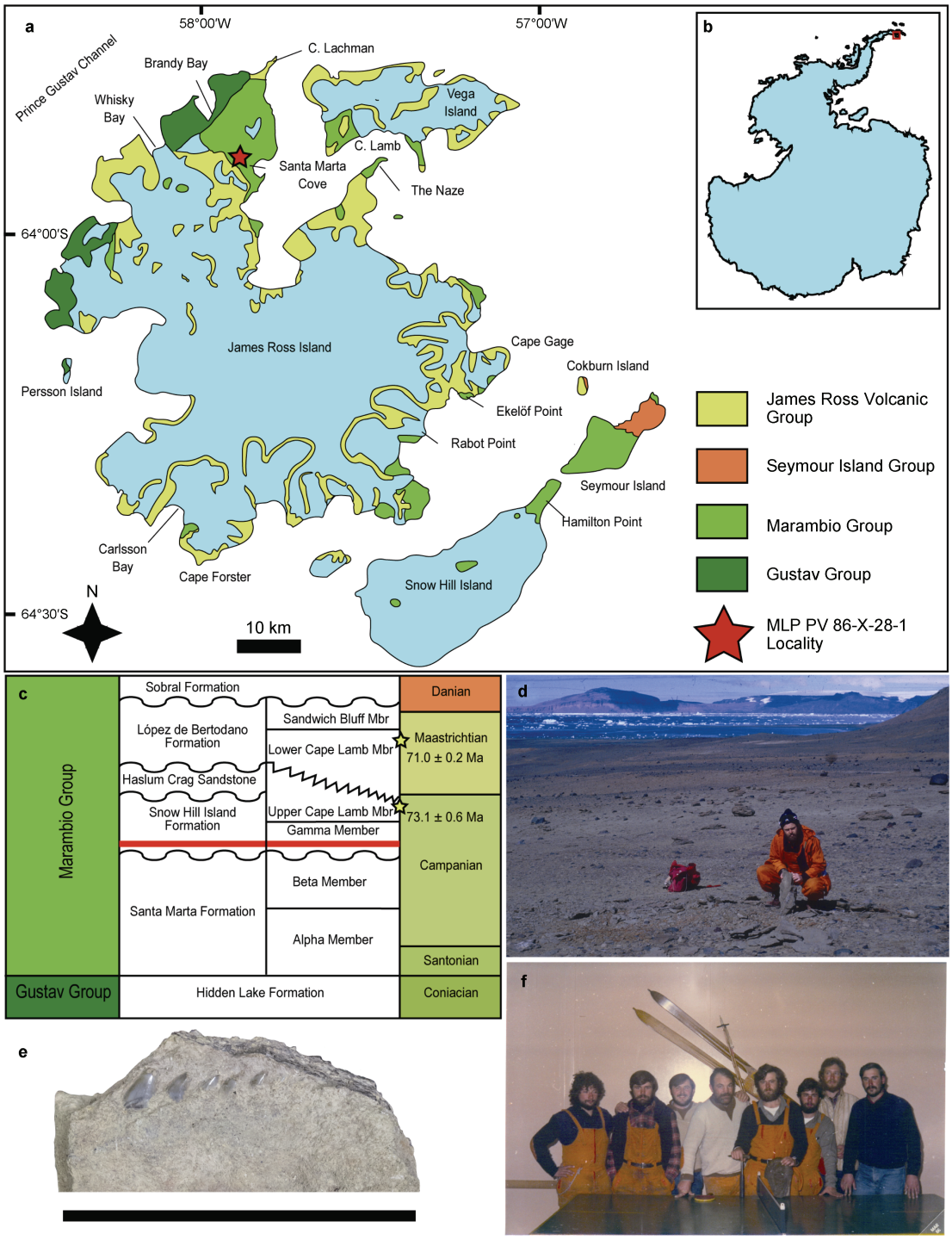

Figure 1 Geographical and geological information of the precedence of MLP-PV 86-X-28-1. **a**, map of the James Ross Island group, showing the geological cartography, the main islands and fossiliferous locations and the location of discovery of MLP-PV 86-X-28-1; **b**, situation of the James Ross Island group within the Antarctic Peninsula; **c**, geochronological table showing the main geological groups, formations and members of the outcrops in the northwest part of the James Ross Basin, including the approximate horizon of precedence of MLP-PV 86-X-28-1; **d**, Eduardo Olivero, from the IAA, posing on the quarry of *Antarctopelta oliveroi* in 1986; **e**, part of the marine fauna associated to MLP-PV 86-X-28-1, including the Hexanchiformes *Notidanodon* sp.; **f**, crew of the IAA expedition in the summer of 1986, from left to right: Ricardo Roura, Jorge Strelin, Jorge Amat, Jorge M. Buirás, Eduardo Olivero, Ernesto Martino, Roberto Scasso and Alejandro López Angriman. The map was redrawn from Milanese et al. (2020). The chronostratigraphic information is based on the proposals of Roberts et al. (2014), Lamanna et al. (2019), Milanese et al. (2020). The photographies were kindly provided by Marcelo Reguero (MLP). The scale bar for *Notidanodon* is 5 cm.

The trees stored in memory were then analyzed in a second round of searching. The outgroup used was *Lesothosaurus*, and the characters were considered with equal weight. For the identification of wildcard taxon, IterPCR was used (Pol and Escapa, 2009), to improve the resolution in the consensus tree.

4 Systematic paleontology

Dinosauria Owen, 1842
Ornithischia Seeley, 1888
Thyreophora Nopcsa, 1928
Ankylosauria Osborn, 1923
Parankylosauria Soto-Acuña et al., 2021
Antarctopelta oliveroi Salgado and Gasparini, 2006

Material—MLP-PV 86-X-28-1, partial skeleton comprising a fragment of the left dentary with one tooth in eruption; at least five isolated cheek teeth; one anterior cervical vertebra; a cast from sediment imprints of three articulated mid cervical vertebrae (missing); one posterior cervical vertebra; a synsacrum preserving two fused dorsosacral centra (presacral rod), and a sacrum preserving 3 sacral centra; three fragmentary anterior to mid caudal vertebrae; four mid to posterior caudal vertebrae, fragments of ribs, the left scapular girdle including the coracoid an the anterior portion of the scapula; a distal fragment of a radius; a possible manual phalanx; portions of the left ilium including part of the supracetabular process and a fragment of the base of the preacetabular process; the proximal and distal epiphysis of almost all metatarsals, being the most complete the right metapodials; two pedal phalanges of different morphotypes; dorsal and/or costal osteoderms, some of them closely appressed to the dorsal ribs; at least three fragments of the sacral shield; and at least two types of flat osteoderms with a large inner concavity that conform part of the caudal weapon; several ossicles including pieces of rock with them in situ. Additionally, there are several maxillary teeth, dentary fragments, a possible maxilla, vertebral centra, an epiphysis of metatarsus, three non-ungual phalanges, one ungual phalanx, bony plates and several ossicles (Coria et al., 2011). However, these elements were not available because they were unpublished (Reguero, 2019, pers. commun.; Herrera, 2023, pers. commun.). The specimen is osteologically and histologically mature (Cerda et al., 2019). For greater detail, see Table S1, with measurements of some *Antarctopelta oliveroi* bony elements.

Locality and horizon—Santa Marta Cove, James Ross Island, Antarctic Peninsula. Gamma Member of Snow Hill Island Formation (upper Campanian). The exact site was relocated in 2009, which made it possible to obtain its geolocation in geographic coordinates (Coria et al., 2011).

Amended diagnosis—Mid-size ankylosaur with a total length estimated of 4 m, which possess the following combination of characters: asymmetrical teeth cheek with at least 7 denticles in the mesial border, with marked vertical ridges confluents with the denticles in the lingual side and ornamented cingulum with fine striations; unfused scapular girdle; metatarsal IV with a proximal epiphysis noticeably wider than the rest of the metatarsals; well-marked striations present in the supracetabular shelf; sacral shield filling the space between both ilia, covering the sacral neural spines, ornamented with several irregular sulci and pits; presence of intradermal ossicles of around 8 mm of diameter.

Antarctopelta oliveroi can be differentiated from *Stegouros* in the following traits: dentary rami lower than those of *Stegouros*; proportionally shorter and wider dorsosacral vertebrae; lower height of the sacral centra; different texture in the sacral shield, being the ornamentation composed of deep channels together with rugosities. Added to the above is the larger size of *Antarctopelta*, which could be twice the size of *Stegouros*. *Antarctopelta* also differs from *Patagopelta* in that the latter has varied morphotypes of osteoderms, including the presence of scutes with concave base, spines and a different shape of the caudal plates, being dorsally convex and ventrally flat and hollow in the base, in the case of *Antarctopelta*, while *Patagopelta* possess plates of flat surfaces in both sides and, fused plates with the crest obliquely oriented. It differs from *Kunbarrasaurus* in the higher number of denticles per tooth in *Antarctopelta* than *Kunbarrasaurus*, the shape of the supracetabular process, which is not subcircular in the later taxon, the thickness of the preacetabular process, which is greater in *Kunbarrasaurus*. The absence of cervical half-ring osteoderms in *Antactopelta* could be another difference. However, the presence of this type of osteoderms could be affected for taphonomy. Among South American ankylosaurs, only in *Patagopelta* the presence of strange cervical half-rings has been described, however there is no direct evidence of association between these osteoderms with cervical vertebrae, and their morphology could be more compatible with a caudal position. Additionally, it could be argued that some of these characters change ontogenetically, however the specimens compared are osteologically mature. Thus far, skeletochronology studies in *Stegouros* are pending, but are beyond the scope of this work.

5 Description

5.1 Dentary

The preserved fragment of the left dentary corresponds to the mid-posterior zone of the dentary. There is no preservation for the contact for post-dentary bones. In labial view, an ornamented surface can be observed, with at least 4 main foramina, 3 of them aligned in the upper part (just below to the alveoli) and one restricted to the lower part, near to an elevated area on the labial surface. On the lower anterior edge of the bone, a fracture exposes the meckelian groove (Figure 2a). In occlusal view, 8 alveoli are preserved,

with the medial wall of each partially eroded. The fourth alveolus (in anterio-posterior direction) preserves a tooth in situ (Figure 2b). The alveoli are oval, with the long axis disposed in the labio-lingual direction. Ventrally, the bone has a long oblique fracture, but the meckelian groove can be observed as a well-defined canal. The lingual surface of the dentary is smoother than the labial one (Figure 2c), and the alveolus with the tooth in situ lacks the lingual wall completely (possibly due preparation with the objective of better observing the tooth).

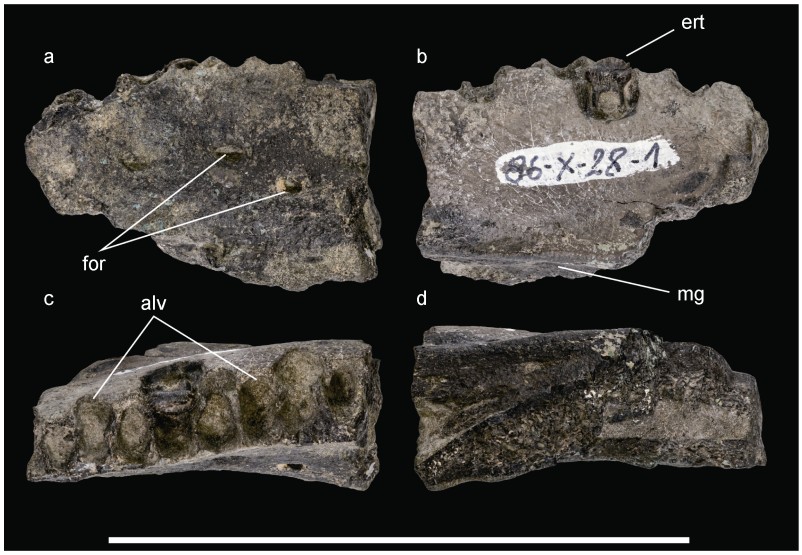

Figure 2 Mandible of MLP-PV 86-X-28-1. **a**, dentary fragment of the left ramus in labial view; **b**, dentary fragment in lingual view; **c**, dentary fragment in occlusal (upper) view; **d**, dentary fragment in ventral view. Anatomical abbreviations: alv, alveoli; ert, erupted tooth; for, foramina; mg, meckelian groove. Scale bar = 10 cm.

5.2 Teeth

In addition to the in-situ tooth in the dentary, five other isolated teeth are preserved, three of them including the crown, the cingulum and part of the root. The crowns are expanded respect to the rest of the teeth and have a foliar asymmetrical shape, with more denticles in the mesial side than the distal side (Figure 3). In the two best preserved teeth there is a central cusplet that is well differentiated from the rest of the denticles, which is distally displaced. The cingulum, intended as the mesiodistal and labiolingual expansions of the crown base (Hendrickx et al., 2015), is conspicuous, being widened in mesio-distal views and possessing two marginal ridges, having different morphologies in the labial and lingual sides. The inferred position and lateralization of *Antarctopelta* teeth are confirmed with the new information of the two in situ teeth in the dentary of *Stegouros elengassen* (Soto-Acuña et al., 2021).

The labial side have an asymmetrical cingulum in transverse sense, with three elevations (in apico-basal direction), one mesial (well-defined), one central, and one distal (less developed), giving a sinuous aspect to the cingulum (Figure 3). The cingulum is ornamented with fine vertical striae, which begin in the basal portion together with transversal undulations, and end in the upper part of the cingulum, without continuation with the furrows of the crown (Figure 3). The previously mentioned marginal ridges are projections of the cingulum that reach the edges of the crown, giving the appearance of a denticle, known as pseudodenticles (Figure 3).

The rest of the crown is at least twice as tall as the cingulum, having well marked ridges and furrows, which are confluent with the denticles. A prominent central and vertical bulge is observed, connecting the cingulum with the most apical portion. The apical denticle is more elevated than the other denticles. Below the cingulum, the root is wider than the rest of the crown and has a bulbous shape.

The lingual side shows a very different morphology (Figure 3), having a more elevated cingulum, which is apically arched and almost as tall as the crown. There are also fine vertical striations over the cingulum, but these are more sinuous than those of the lingual side. The ridges and furrows are less marked, particularly those of the center of the crown. There are no signs of a vertical bulge. In mesial or distal views, its sinuous appearance of the teeth can be observed, with roots lingually directed.

5.3 Cervical vertebrae

5.3.1 Anterior cervical vertebrae

Only one anterior cervical is preserved. The neural arch is incomplete, lacking most pre- and post-zygapophyses and the neurapophysis. The centrum is wider than length and height. The articular faces are slightly amphiplatyan, with a slightly protruding border (Figure 4). In anterior aspect, the neural canal has a quadrangular shape, having half the height of the centrum (Figure 4). The ventral part of the centrum is eroded, exposing the inner tissue of

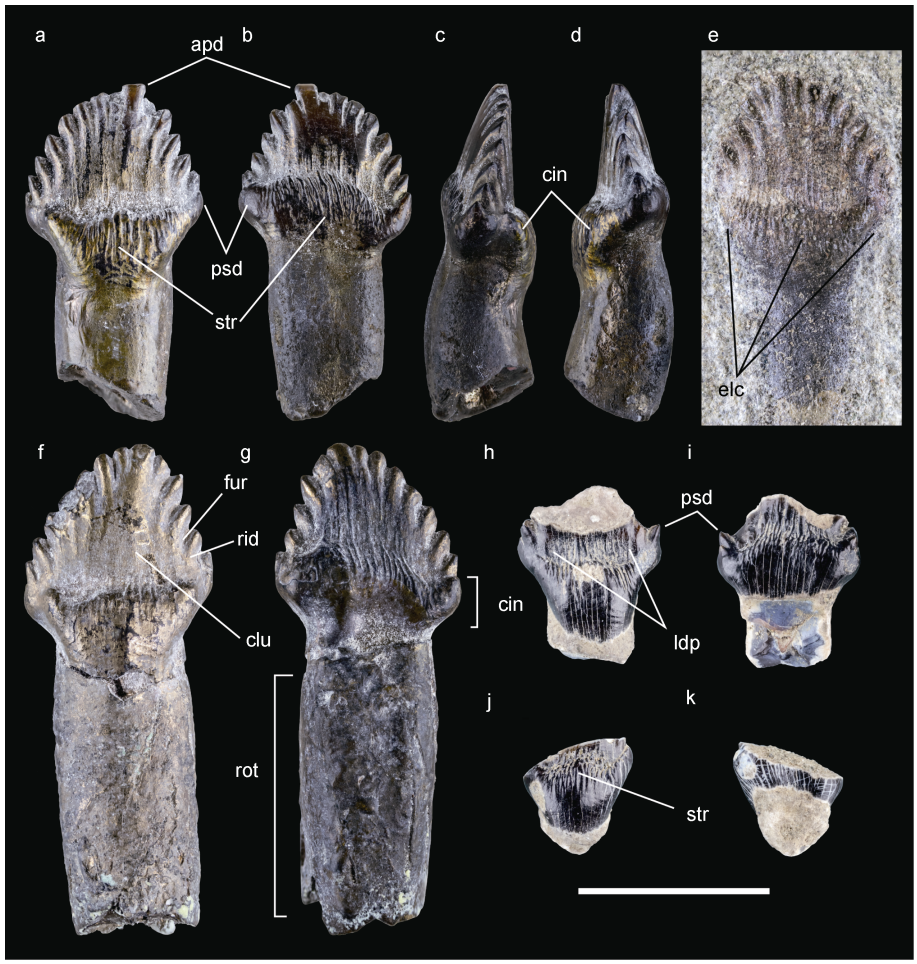

Figure 3 Teeth of MLP-PV 86-X-28-1. Well-preserved tooth No.1 in lingual (**a**), labial (**b**), mesial (**c**), and distal views (**d**); **e**, tooth No. 3 still in the rock matrix in labial view; **f**, lingual view of tooth No. 4, with part of the root; **g**, labial view of tooth No. 4; **h**, labial view of tooth No. 4; **i**, lingual view of tooth No. 4; **j**, labial view of fragmentary tooth No. 5; **k**, lingual view of fragmentary tooth No. 5. Anatomical abbreviations: apd, apical denticle; cin, cingula; clu, central lump; elc, elevations of the cingulum; fur, furrow; ldp, lateral depressions; psd, pseudodenticle; rid, ridge; rot, root; str, striations. Scale bar = 1 cm.

the centrum. At least a pair of foramina are observed on the ventral side. Postzygapophyses are slightly insinuated but mostly eroded (Figure 4). In lateral view it can be observed that the preserved neural arch is more elevated in the posterior portion. There is no sign of suture between the neural arch and the centrum, indicating an osteologically mature individual.

5.3.2 Mid cervical vertebrae

These are preserved as a cast of imprints left in sediments after erosion/loss of the original vertebrae, which were in articulation. All of them are anterioposteriorly short in relation to its height and width, and approximately as wide as they are tall. The neural arches are partially preserved, and the last vertebra shows prezygapophyses near each other, postzygapophyses, and a low spine (Figure 5). The neural canal is still circular in shape. The articular faces of the preserved centra are amphicoelous, with a well-marked border. The shape of the centra in articular view is slightly polygonal, probably due to the existence of a diapophysis migrating to the neural arch (being well visible in lateral view). The diapophyses are circular in cross-section and point laterally. Large concavities are developed on the lateral sides, anterior to the transverse process and below the neural arch (Figure 5).

5.3.3 Posterior cervical vertebra

This vertebra is larger in comparison to the previous cervicals elements. It is almost complete, except for a fracture on the left side of the centrum (Figure 6). The neural arch is still low, with a likely short neural spine in relation to the neural arch height, a wide lateral space for the prezygapophyses and postzygapophyses that are closer to each other, but still separated. The transverse process is attached to the peduncles of the neural arch; hence this vertebra is transitional to the dorsals. These point slightly in dorsolateral direction, indicating the beginning of the inclination of the transverse process of the dorsal vertebra.

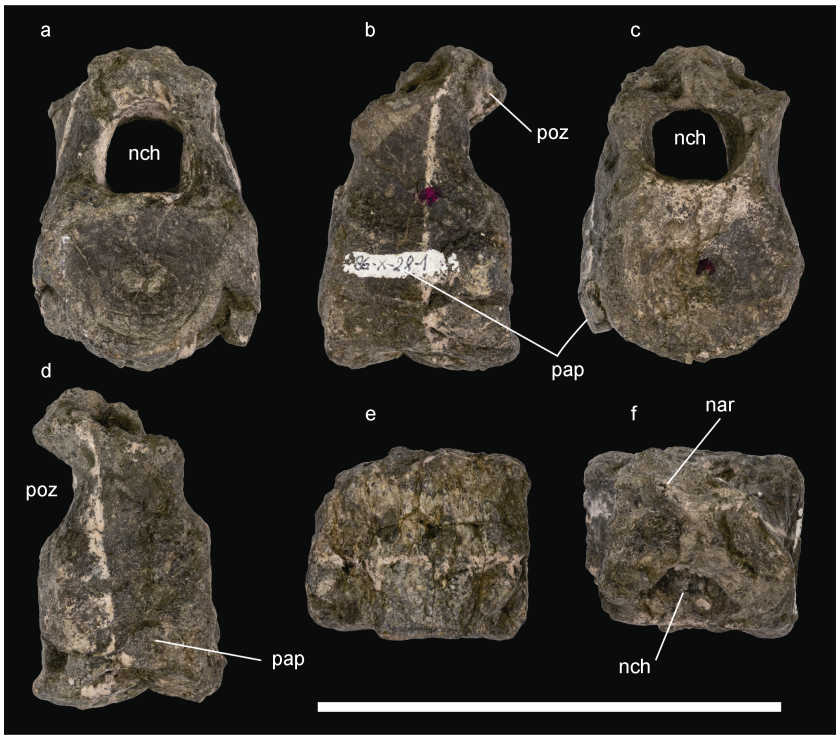

Figure 4 Anterior cervical vertebra of MLP-PV 86-X-28-1. **a**, cervical vertebra in anterior view; **b**, cervical vertebra in left lateral view; **c**, cervical vertebra in posterior view; **d**, cervical vertebra in right lateral view; **e**, cervical vertebra in ventral view; **f**, cervical vertebra in dorsal view. Anatomical abbreviations: nar, neural arch; nch, neural canal; pap, parapophysis; poz, postzygapophysis. Scale bar = 10 cm.

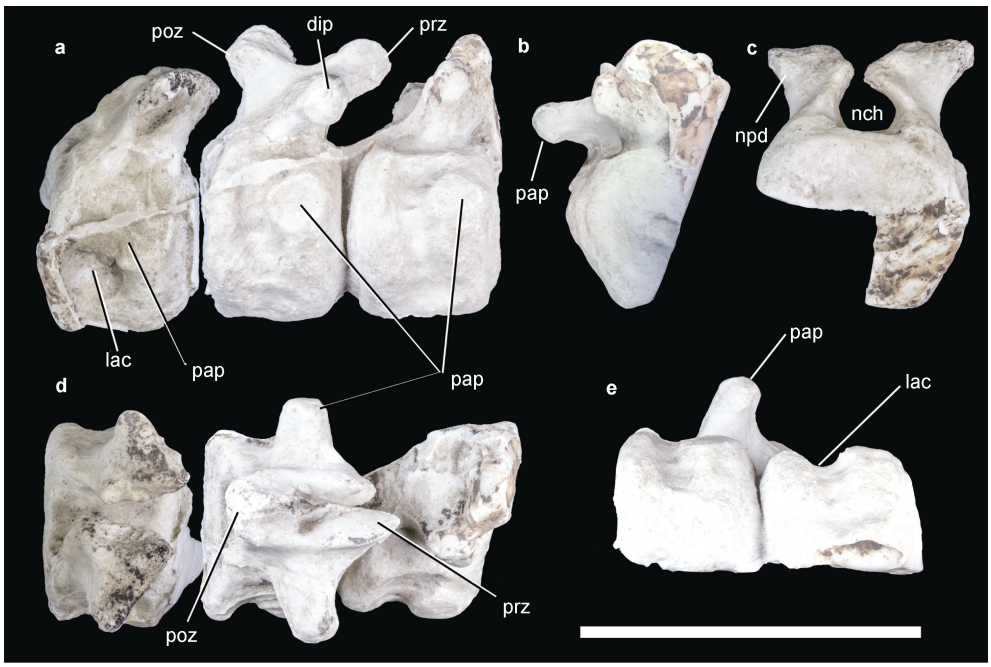

Figure 5 Cast of the mid cervical vertebra of MLP-PV 86-X-28-1. **a**, three mid-cervical vertebrae in left lateral view; **b**, first mid-cervical vertebra of the sequence in anterior view; **c**, last mid-cervical vertebra of the sequence in posterior view; **d**, three mid-cervical vertebrae in dorsal view; **e**, first and second mid-cervical vertebrae of the sequence in ventral view. Anatomical abbreviations: dip, diapophysis; lac, lateral excavation; nch, neural canal; npd, neural peduncle; pap, parapophysis; poz, postzygapophysis; prz, prezygapophysis. Scale bar = 10 cm.

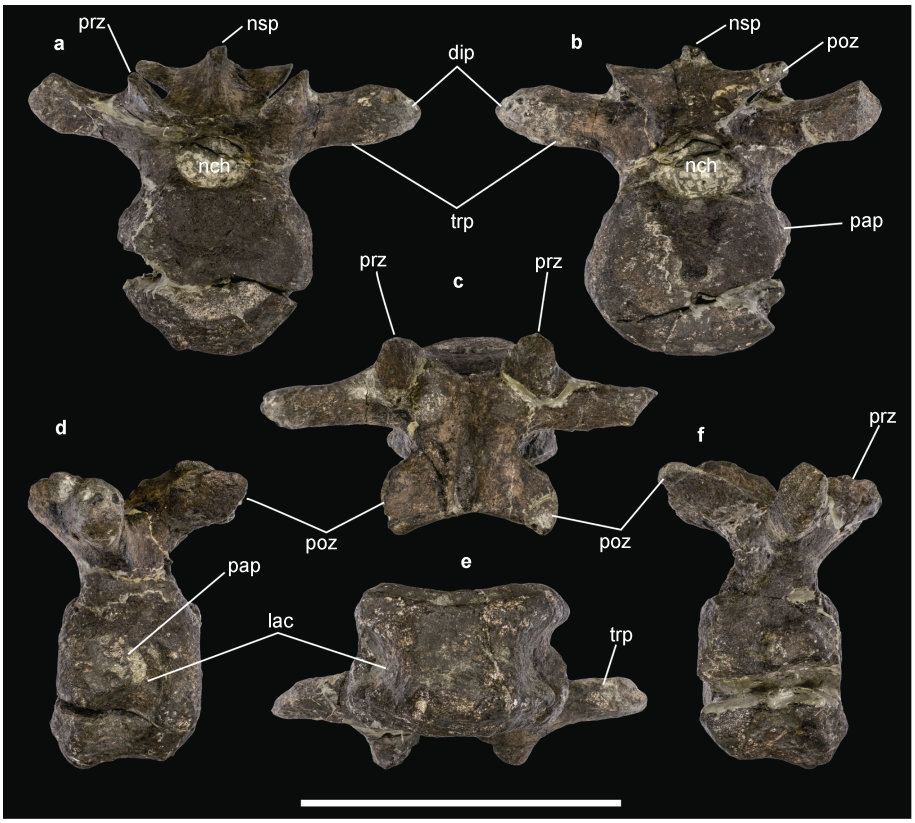

Figure 6 Posterior cervical vertebra of MLP-PV 86-X-28-1. **a**, cervical vertebra in anterior view; **b**, cervical vertebra in posterior view; **c**, cervical vertebra in dorsal view; **d**, cervical vertebra in left lateral view; **e**, cervical vertebra in ventral view; **f**, cervical vertebra in right lateral view. Anatomical abbreviations: dip, diapophysis; lac, lateral excavation; nsp, neural spine; pap, parapophysis; poz, postzygapophysis; prz, prezygapophysis; trp, transverse process. Scale bar = 10 cm.

The neural canal is circular. The centrum is polygonal, slightly amphiplatyan and forming a circular articulation area. The lateral side is excavated, except for a slight development of bone, the parapophysis. The lateral excavation is continuous with a ventral constriction of the centrum. The numerical position among the cervicals is uncertain, however this element shares the same traits with the inferred cervical number eight of *Stegouros* (Soto-Acuña et al., 2021).

5.4 Dorsosacral vertebrae

Two fused dorsosacral centra are preserved, also known as the presacral rod. The anterior one has an oval shape in the articular face, and there is no evidence of anterior fusion anterior to this one (Figure 7). The second vertebra is badly preserved, lacking the most posterior portion of the articular face, which probably was fused with another dorsosacral or the sacral vertebrae. If a comparison with *Stegouros* is made, the second vertebra could be the last one of the presacral rod, articulating or fusing with the sacral vertebrae. The ventral surface is rounded, without grooves or keels, however there is a transversal elevation at the same level of the fusion between the two centra. They are significantly more robust and proportionally shorter than the equivalent presacral rod of *Stegouros*.

5.5 Sacral vertebrae

Three sacral vertebrae of the synsacrum are preserved. They have very depressed centra, contrasting with the presacral rod, and preserve only part of the peduncles of each neural arch (Figure 7). Only the base of the transverse processes is preserved, being big and wide in proportion to each sacral vertebra. These processes are laterally directed, except for the most posterior preserved sacral vertebra, where the transverse processes point slightly to posterior. All the sacrum is broken longitudinally, and the most posterior vertebra also lacks the articular face or contact with the next vertebra. A half of this vertebra, undescribed until now, was discovered in the collection. If the sacral formula is similar to *Stegouros*, one more sacral can be expected posteriorly. On the other hand, at least one centrum of the presacral rod is missing, which would connect with the sacrum. The ventral face is almost flat to convex, without presence of keels or sulcus. The most anterior sacral seems to be the first one, based on the well-developed concave-convex articulation suitable for the

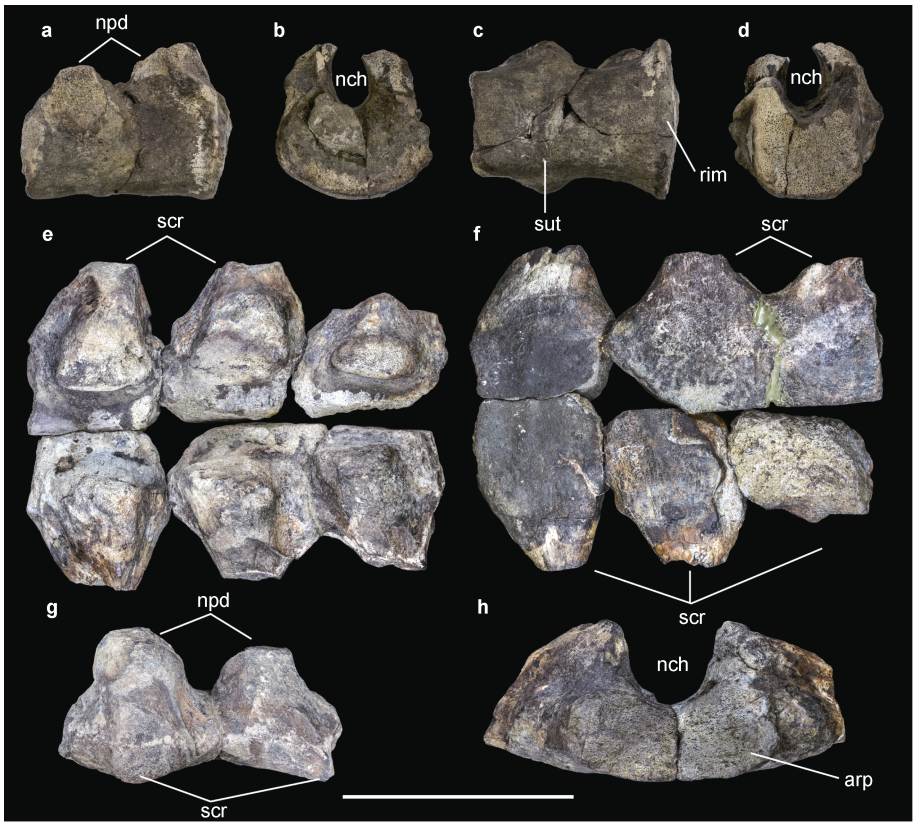

Figure 7 Synsacral vertebra of MLP-PV 86-X-28-1. **a**, dorsosacral vertebrae in right lateral view; **b**, first dorsosacral vertebra in anterior view; **c**, dorsosacral vertebrae in ventral view; **d**, second dorsosacral vertebra in posterior view; **e**, sacral vertebrae in dorsal view; **f**, sacral vertebrae in ventral view; **g**, two most anterior sacral vertebrae in right lateral view; **h**, anterior sacral vertebrae in anterior view. Anatomical abbreviations: arp, articulation for presacral rod; nch, neural canal; npd, neural peduncle; rim, rim; scr, sacral rib; sut, suture. Scale bar = 10 cm.

presacral rod. This articulation is almost twice as wide as it is tall, different from the condition in *Stegouros*, where these measures are equivalent.

5.6 Caudal vertebra

Around eight vertebrae are counted, however many of them are badly preserved. The fragments of three vertebrae show that the anterior ones have centers that are shorter than the width, as well as wider than length (Figure 8). The transverse processes are well-developed but broken, so there is no information about the direction in which they point. The ventral surface has a longitudinal furrow, which probably increased in size towards caudal. The best preserved anterior caudal was mistaken with a pygal vertebra of a mosasaur (Arbour and Currie, 2016), however the articular face is not procoelic like in these squamates (Estes et al., 1988). Only one neural peduncle is preserved, but incomplete.

There are at least four mid to posterior vertebrae in different states of preservation. The most completely preserved one shows a bizarre morphology, with a very flat centrum, antero-posteriorly elongated and dorso-ventrally flat transverse processes, which almost reach the posterior border of the centrum, wide ventral furrows, and a mid-constriction (Figure 8). No neural arch is preserved; however, the floor of the neural canal can be observed in some cases. One of the most interesting features is the presence of ossified tendons parallel to the axis, which were recognized by Salgado and Gasparini (2006) and Rozadilla et al. (2021). These vertebrae were described as “binocular-shaped” cervicals and referable to Elasmosauridae by Arbour and Currie (2016); however, the morphology of cervical vertebrae in the Elasmosauridae is very distinctive, including the presence of a ventral pair of foramina, together with a well-developed lateral crest and, in euelasmosaurs, a very narrow ventral notch that gives the binocular shape to the articular faces (O’Gorman, 2020; Welles, 1952). The anatomy of the “macuahuitl” or caudal weapon of *Stegouros*, shows that the inner caudal vertebrae of this section are compatible with the posterior caudal vertebrae of *Antarctopelta*. Therefore, there are no doubts about the identity of the caudal vertebrae of this taxon.

5.7 Ribs

There are around eight fragments of ribs, probably from the dorsal portion of the animal, being a L-shaped in

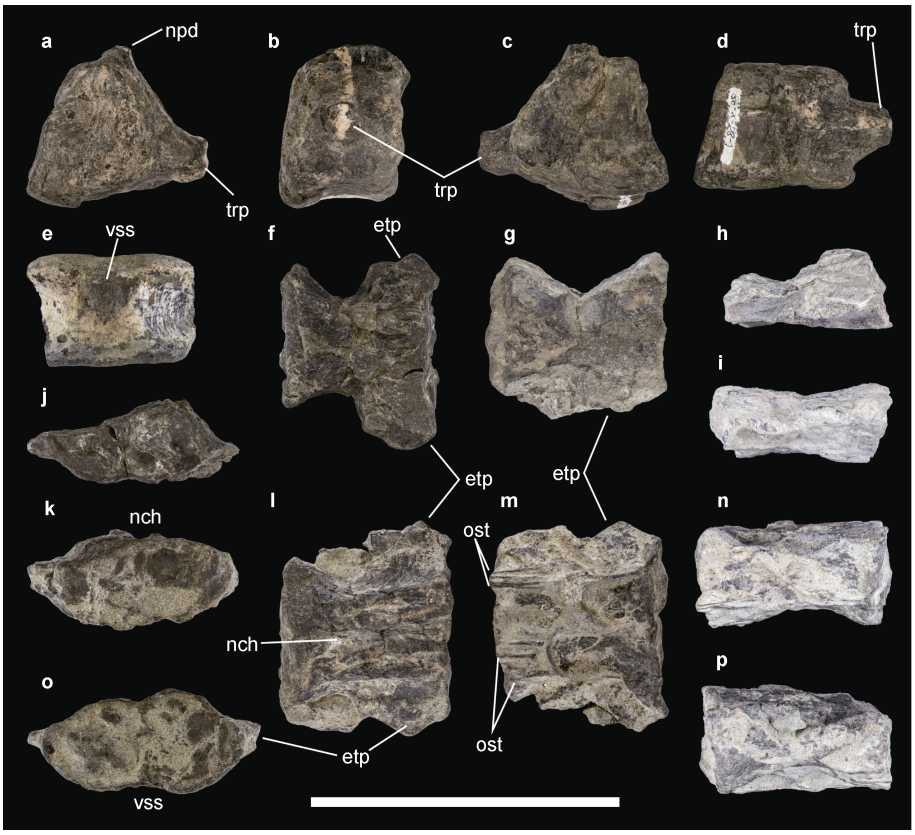

Figure 8 Selected caudal vertebrae of MLP-PV 86-X-28-1. Due to bad preservation, the same view for all centra are no available. The numbering given to the vertebrae is only for distinction, they do not indicate anatomical position: **a**, half of anterior caudal vertebra No. 1 in anterior view; **b**, half of anterior caudal vertebra No. 1 in left lateral view; **c**, half of anterior caudal vertebra No. 1 in posterior view; **d**, half of anterior caudal vertebra No. 1 in ventral view; **e**, fragment of anterior to mid caudal vertebra No. 2 in ventral view; **f**, posteriormost caudal vertebra No. 3 in dorsal view; **g**, posteriormost caudal vertebrae No. 4 in dorsal view; **h,** posteriormost caudal vertebrae No. 3 in left lateral view; **i**, posteriormost caudal vertebra No. 4 in left lateral view; **j**, posteriormost caudal vertebrae No. 3 in posterior view; **k**, posteriormost caudal verterbra No. 5 in anterior view; **l**, posteriormost caudal verterbra No. 5 in dorsal view; **m**, posteriormost caudal verterbra No. 5 in ventral view; **n**, **p**, posteriormost caudal vertebra No. 5 in left and right lateral views respectively; **o**, posteriormost caudal vertebra No. 5 in posterior view. Abbreviations: etp, elongated transverse process; nch, neural canal; npd, neural peduncle; ost, ossified tendons; trp, transverse process; vss, ventral sulcus. Scale bar = 10 cm.

cross-section, like *Stegouros*. Two of these fragments are associated with oval low-keeled osteoderms, which will be discussed later. Also, marks of sacral or presacral ribs are present in the ilia fragments and the sacral shield.

5.8 Coracoid

The coracoid was not originally recognized in previous descriptions. The shape of this element is quadrangular, however part of the surface in the anterior and dorsal borders are eroded, thus a precise contour cannot be deduced (Figure 9). A coracoid foramen is preserved, but the most anterior border is missing due to erosion. This foramen is in the anterior portion of the coracoid (presuming that not much of the bone was eroded in the anterior margin). The glenoid articulation, located in the ventroposterior edge, has almost the same length the articulation for the scapula. There is no fusion with the scapula, which is typical for advanced ankylosaurs (Vickaryous et al., 2004).

5.9 Scapula

The scapula of the right side preserves the most anterior portion, lacking the scapular blade. The anterior zone articulates with the coracoid, while the immediately posterior dorsal border is more elevated, giving a more robust aspect to the bone. A deltoid crest is not visible due to erosion (Figure 9). The preserved ventral border contributes entirely to the glenoid fossa, so the glenoid is conformed to a greater degree by the scapula than by the coracoid. In lateral view, some sinuous striations can be observed on the surface. There is no trace of humerus, however, the size of the glenoid indicates that the humeral head was well-developed.

5.10 Radius

This element, not previously identified, consist only of the proximal epiphysis of a radius (Figure 9). The subtriangular

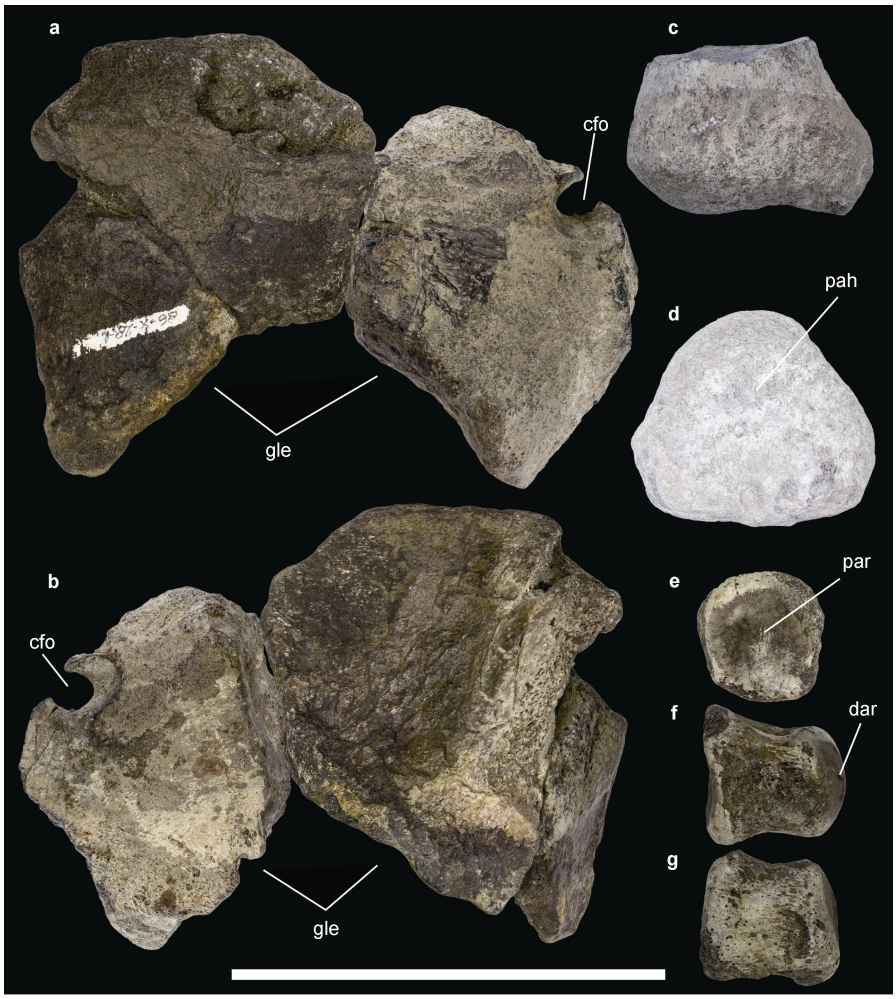

Figure 9 Pectoral girdle and forelimb elements of MLP-PV 86-X-28-1. **a**, articulated right scapular girdle, including the anterior part of the scapula and the posterior part of the coracoid in lateral view; **b**, scapular girdle in medial (inner) view; **c**, proximal epiphysis of radius in lateral view; **d**, proximal epiphysis of radius in distal view; **e**, possible manual phalanx in proximal view; **f**, possible manual phalanx in lateral view; **g**, possible manual phalanx in dorsal view. Anatomical abbreviations: cfo, coracoid foramen; dar, distal articulation; gle, glenoid; pah, proximal articulation for humerus; par, proximal articulation. Scale bar = 10 cm.

section and shape of the epiphysis, its diameter slightly more robust than a metapodial, and its resemblances with the radius of *Stegouros*, allows its identification.

5.11 Manual phalanx

One non-ungual phalanx, possibly of the manus, is preserved. This conclusion is based on a comparison with the manus of *Stegouros*. The element is tubular in shape, as long as it is wide and tall, and there is a slight constriction in the middle of the phalanx (Figure 9). Both articular faces are flat, lacking condyles, extensor or flexor fossae and collateral pits, indicating a low degree of movement of the digit. The proportions are noticeably minor to the pedal non-ungual phalanx.

5.12 Ilium

The preserved portion of the right ilium corresponds to a segment of the preacetabular process and fragment of the supracetabular and postacetabular process (Figure 10). The preacetabular process is straight and becomes narrower in the anterior end. Unfortunately, there is no more information about the direction and inclination of this process, nonetheless, judging from the ilium of *Stegouros*, *Kunbarrasaurus* and other parankylosaurs (Molnar et al., 1996; Soto-Acuña et al., 2021), the preacetabular process pointed in anterolateral direction and probably also ventrally.

The posterior fragment is bigger than the first fragment, and it can be recognized by the contour of its lateral edge and the ornamentation of the edge. The contour is almost straight, except for the most anterior zone where a prominent shelf is developed, just over the inferred acetabulum (non-preserved). All the edges have marked striations like in *Stegouros*, which become even more conspicuous in the anterior shelf. The rest of the bone is almost flat, but there are no borders preserved. Judging

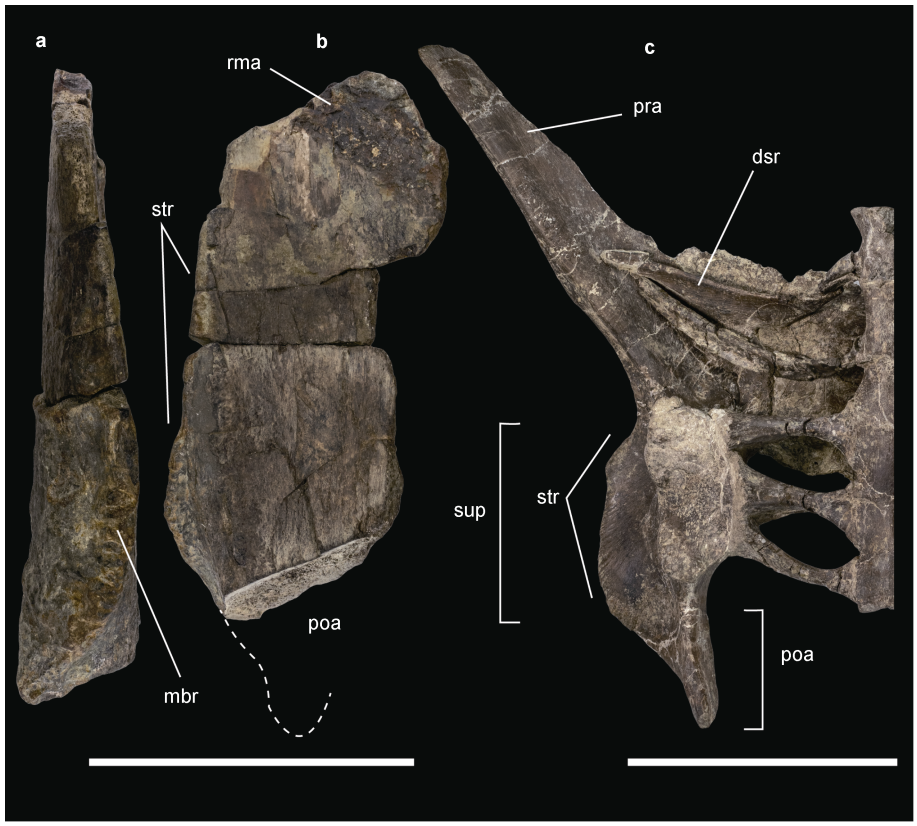

Figure 10 Pelvis of MLP-PV 86-X-28-1. **a**, fragment of preacetabular process of the right ilium in medial view; **b**, fragment of the right ilium preserving the supracetabular and postacetabular processes including the inferred contour of the caudal portion; **c**, left ilium (inverted) of *Stegouros elengassen* for comparison. Anatomical abbreviations: dsr, dorsosacral rib; mbr, medial border; poa, postacetabular process; pra, preacetabular process; rma, rib marks; str, striations; sup, supracetabular process. Scale bars = 10 cm.

from the shape of the pelvis in *Stegouros*, the most posterior end should be the base of the postacetabular process. The anterior portion, which ends in a broken border, has no contact with the preacetabular process. However, a close inspection allows to observe one straight mark, obliquely oriented in the ventral surface. This mark is here interpreted as the contact with a sacral, or more probably a dorsosacral rib, which commonly touch (or are even fused) with the ilia in ankylosaurs (Carpenter et al., 2013) and is also observable in *Stegouros* (Soto-Acuña et al., 2021).

5.13 Metatarsals

Several pieces of epiphyses have been identified as metatarsals from both hindlimbs, including at least evidence for five metatarsals (Salgado and Gasparini, 2006). The better-preserved side is the right, where the metatarsal II is represented by the distal end and the metatarsals III and IV by both ends. The proximal epiphysis of the metatarsal IV is easily recognizable for the subtriangular shape in proximal view and the proximo-lateral expansion (Figure 11), both present in *Stegouros*. The contact of the metatarsal III and IV in proximal view fits well. Distally, however, there is no evidence of clear contact between the epiphysis, probably due to the different relative position of these in proximo-distal direction. Despite the massive shape of some of these epiphyses (Salgado and Gasparini, 2006), the broken ends indicate that the shafts of these bones were slender. It is uncertain if the length of the metapodials is as thin or more robust than those of *Stegouros*.

Two little fragments of an epiphysis probably correspond with the metacarpal I of the foot, however there is no connection between these two pieces. The flat articulation of the proximal end indicates that this possible metacarpal is from the left foot.

5.14 Pedal phalanges

A phalanx very compressed medio-distally was preserved and isolated. There is no information that allows to assign it to the left or right foot, but the flattened shaped allows to propose several positions within the foot. In *Stegouros*, the ancestral phalangeal formula for Ornithischia is retained (2-3-4-5-0), nonetheless, in the digit III, the phalanx III-2 and III-3 are the most flattened, and in the digit IV all the non-ungual phalanges are also flattened. The articular faces of the phalanx of *Antarctopelta* are flat to slightly concave. In section, the phalanx is almost twice as wide as it is tall.

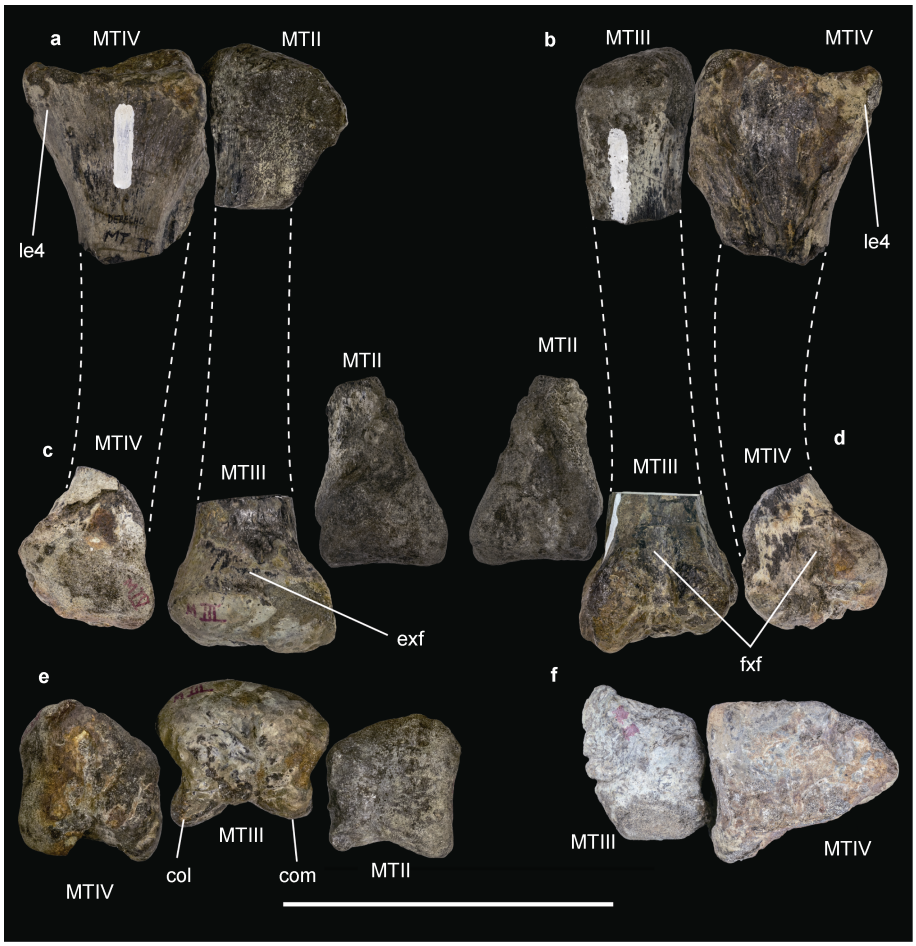

Figure 11 Metatarsals of MLP-PV 86-X-28-1. **a**, proximal epiphyses of the metatarsals III and IV of the right foot in dorsal view; **b**, proximal epiphyses of the metatarsals III and IV of the right foot in plantar view; **c**, distal epiphyses of the metatarsals II, III and IV of the right foot in dorsal view; **d**, distal epiphyses of the metatarsals II, III and IV of the right foot in plantar view; **e**, distal epiphyses of the metatarsals II, III and IV in distal view; **f**, proximal epiphyses of the metatarsals III and IV in proximal view. Anatomical abbreviations: col, lateral condyle; com, medial condyle; exf, extensor fossa; fxf, flexor fossa; le4, lateral expansion of MTIV; MTII, metatarsal 2; MTIII, metatarsal 3; MTIV, metatarsal 4. Scale bar = 10 cm.

5.15 Dorsal osteoderms

At least eight isolated or articulated osteoderms from the dorsal portion of the animal are preserved. Among them, there is a morphotype characterized by being oval, low keeled and highly ornamented by groves and foramina in the external aspect (Figure 12). The inner aspect is irregular, but almost flat, without any concavities. Previously some authors have described fusion between this type of osteoderms with dorsal ribs (Arbour and Currie, 2016; Maidment et al., 2021). A close examination of the material allows to conclude that there is sediment between both elements in the two osteoderms-ribs association, so a fusion can be discarded. Furthermore, one of the rib pieces has an osteoderm with the keel oriented obliquely to the main axis of the rib, indicating that after burial some taphonomical process acted on the skeleton.

A second morphotype, like the anterior one, but with a concave ventral surface, is preserved (Figure 12h). This osteoderm could belong to the dorsal or the anterior caudal zone of the skeleton. Also, in *Stegouros*, a similar osteoderm can be found in close association with the hindlimbs (Soto-Acuña et al., 2021)

5.16 Sacral shield

This is the most unusual kind of dermal armor, because it doesn't have any equivalent in sacral shields of ankylosaurids, nodosaurs and "polacanthines" (Arbour et al., 2011). The armor consists of fragments of dermal bones with a ventral smooth texture and dorsal ornamented surface, somewhat like *Stegouros*, which probably covered the space between both ilia and the sacrum (Figure 13). Stegosauria have a similar sacral shield in the pelvis, however in this case the armor is composed entirely by the dorsal expansion of the sacral ribs (Galton and Upchurch, 2004). Evidence of a composite of polygonal osteoderms in the sacral shield of *Antarctopelta* is absent (contra Arbour and Currie, 2016). On the other hand, some well-marked

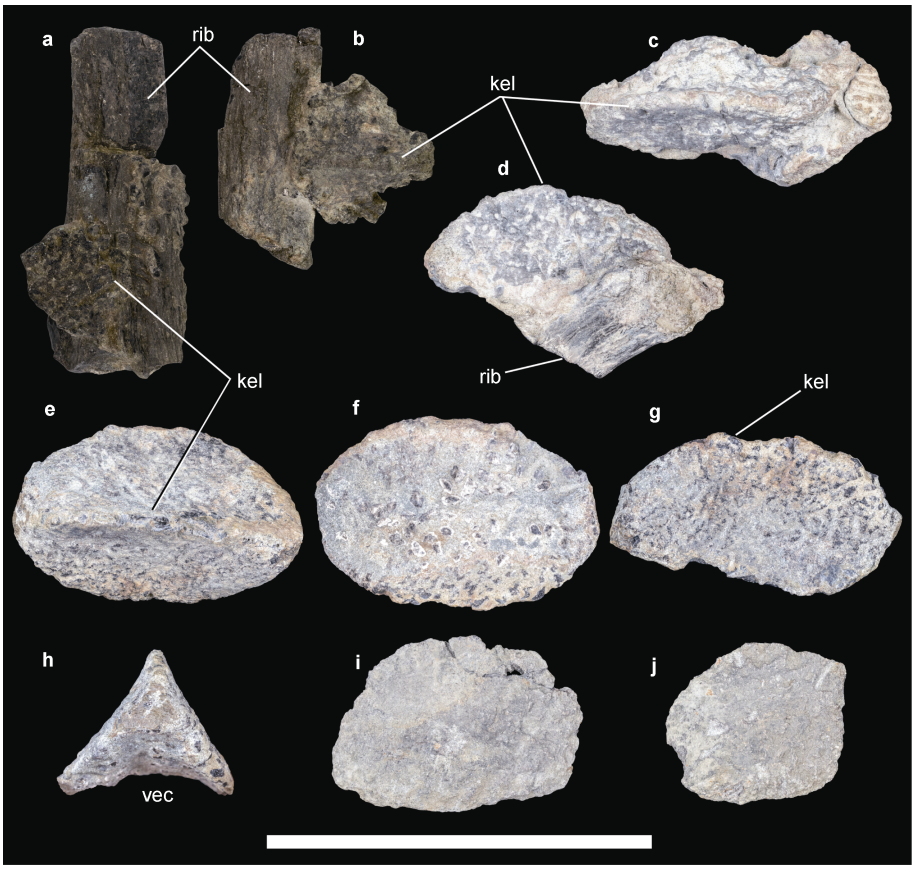

Figure 12 Different kind of body osteoderms of MLP-PV 86-X-28-1. **a**–**b**, low keeled irregular osteoderms associated with ribs; **c**, high keeled elongated osteoderm associated with a bone (rib?) in dorsal view; **d**, high keeled elongated osteoderm in lateral view; **e**, high keeled oval osteoderm in dorsal view; **f**, high keeled oval osteoderm in ventral view (note the flat ventral surface); **g**, high keeled oval osteoderm in lateral view; **h**, another type with high keel osteoderm with concave ventral surface in antero-posterior view; **i**, another type of flat osteoderm without keel in dorsal view; **j**, second flat osteoderm without keel in dorsal view. Anatomical abbreviations: kel, keel; rib, rib; vec, ventral concavity. Scale bar = 10 cm.

furrows and foramina are present in the surface of the bone, and at least one piece possesses a fragment of rib associated or fused to it (Figure 13). This condition is shared with *Stegouros elengassen* (Soto-Acuña et al., 2021) and probably with *Kunbarrasaurus ieversi* (Molnar, 2001) where sacral and some dorsosacral ribs contact with the sacral armor. Another piece of sacral shield has a fused fragment of trabecular bone in the ventral side, which marks a semicircular contour. It is possible that this bone corresponds to the ilium, however the fragmentary nature of the piece does not confirm this possibility.

5.17 Caudal osteoderms

The caudal osteoderms were initially interpreted as cranial bones, including a parietal, supraorbital and quadrato-jugal (Salgado and Gasparini, 2006). The discovery of *Stegouros* revealed the independent evolution of a new type of caudal weapon unlike other ankylosaurs (Arbour and Zanno, 2018), composed of several fused flat osteoderms very concave internally, in the most posterior portion of the tail, and surrounding the most caudal vertebrae. Particularly two elements, the previously referred supraorbital and parietal, fit well with the first and third pair of osteoderms of the caudal weapon of *Stegouros elengassen* (Soto-Acuña et al., 2021). The smallest osteoderm is keeled, convex in both external surface and very concave in the inner surface. The keel is supposed to be aligned with the axial skeleton. The second osteoderm, bigger than the first one, has a flat dorsal surface, while part of the ventral surface (preserved only in the most lateral edge) is convex. Internally there are parallel fibers that could correspond to the antero-posteriorly elongated transverse processes, however articulated material is necessary to confirm this. New flat osteoderm were identified in the specimen that could correspond to the caudal weapon (Figure 14).

5.18 Ossicles

The ossicles are tiny dermal bones varying of subcircular to quadrangular shape that were probably inserted in the dermis of the entire body like interstitial bones (Scheyer and Sander, 2004). There is no evidence of grouping of ossicles surrounding bigger osteoderms, as in

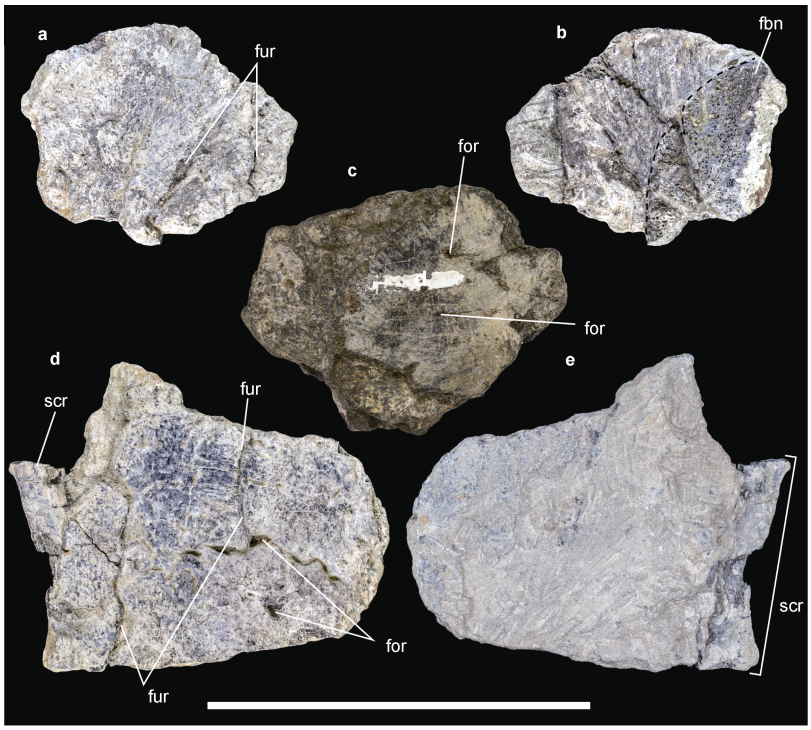

Figure 13 Sacral osteoderms of MLP-PV 86-X-28-1. **a**, thin (5 mm approximately) dermal bone fragment of the sacral shield in dorsal view; **b**, dermal bone fragment of the sacral shield in ventral view; **c**, second fragment of dermal bone of the sacral shield in dorsal view; **d**, third fragment of dermal bone of the sacral shield with sacral rib associated in dorsal view; **e**, third fragment of dermal bone of the sacral shield with sacral rib associated in ventral view. Anatomical abbreviations: fbn, fused bone; for, foramina; fur, furrow; scr, sacral rib. Scale bar = 10 cm.

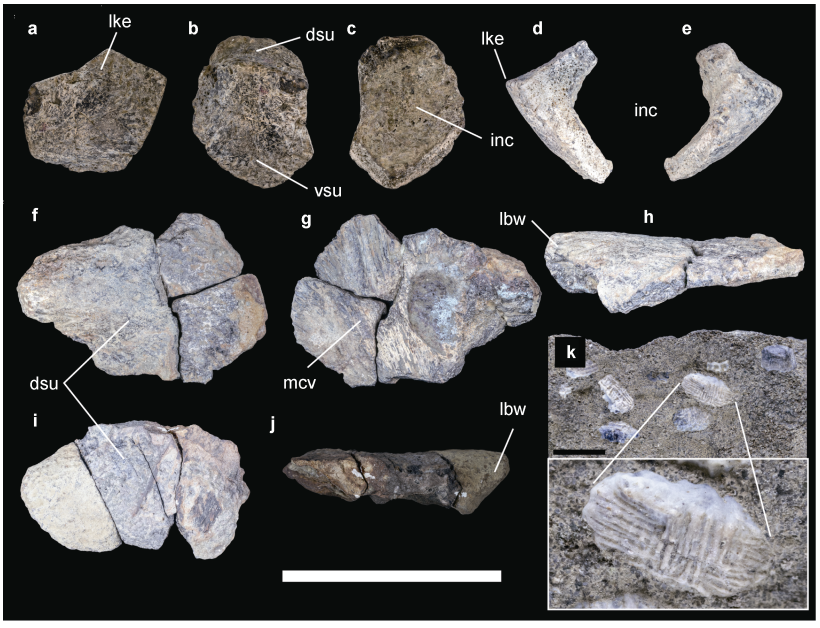

Figure 14 Caudal osteoderms and ossicles of MLP-PV 86-X-28-1. **a**, first type of caudal osteoderm with well-developed keel conforming the first pair of the caudal weapon in dorsal view; **b**, first type of caudal osteoderm in left? lateral view; **c**, first type of caudal osteoderm in inner view; **d**–**e**, first type of caudal osteoderm in anterior and posterior views; **f**, second type of caudal osteoderm of the caudal weapon in dorsal view; **g**, second type of caudal osteoderm with marks of the caudal vertebra in inner view; **h**, second type of caudal osteoderm in lateral view; **i**–**j**, another second type of caudal osteoderm in dorsal and lateral views; **k**, block with a cluster of ossicles preserved in different anatomical positions, with a zoom of a well preserved ossicle of 8 mm in inner view, showing the orthogonal collagen fibers. Anatomical abbreviations: dsu, dorsal surface; inc, inner concavity; lbw, lateral border in osteoderms of the caudal weapon; lke, lateral keel; mcv, mark of caudal vertebra; vsu; ventral surface. Scale bar for **a**–**j**: 10 cm; scale bar for **k**: 1 cm.

Scolosaurus cutleri (Arbour et al., 2014), however there are clusters of ossicles forming structures of irregular shape (Figure 14j). The external surface is full of pits and crests, while the inner side have well marked ridges that forms an orthogonal figure, as in *Stegouros*.

6 Phylogenetic relationships

The initial search returned 10 MPTs of 704 steps in length and values of gg (Rescaled Consistency Index): 0.232. In the second round of branch swapping, 10000 MPTs (maximum limit of trees stored in memory) were obtained. Both strict consensus and majority consensus trees had low resolution in some major clades. Through IterPCR the following taxa were found as wildcard taxa: *Ahsihlepelta*, *Cedarpelta*, *Dongyangopelta*, *Hylaeosaurus*, *Minmi*, *Sauroplites*, *Taohelong*, *Zhejiangosaurus*. Of these, only *Minmi* was not pruned because it is a Gondwanan ankylosaur (Molnar, 1980). The reduced majority consensus tree is shown in Figure 15, where in most of the MPTs an early-diverging Parankylosauria lineage is recovered, this time composed of *Kunbarrasaurus ieversi*, *Patagopelta cristata*, *Stegouros elengassen*, cf. *Kunbarrasaurus* and *Antarctopelta oliveroi*. On the other hand, a clade of

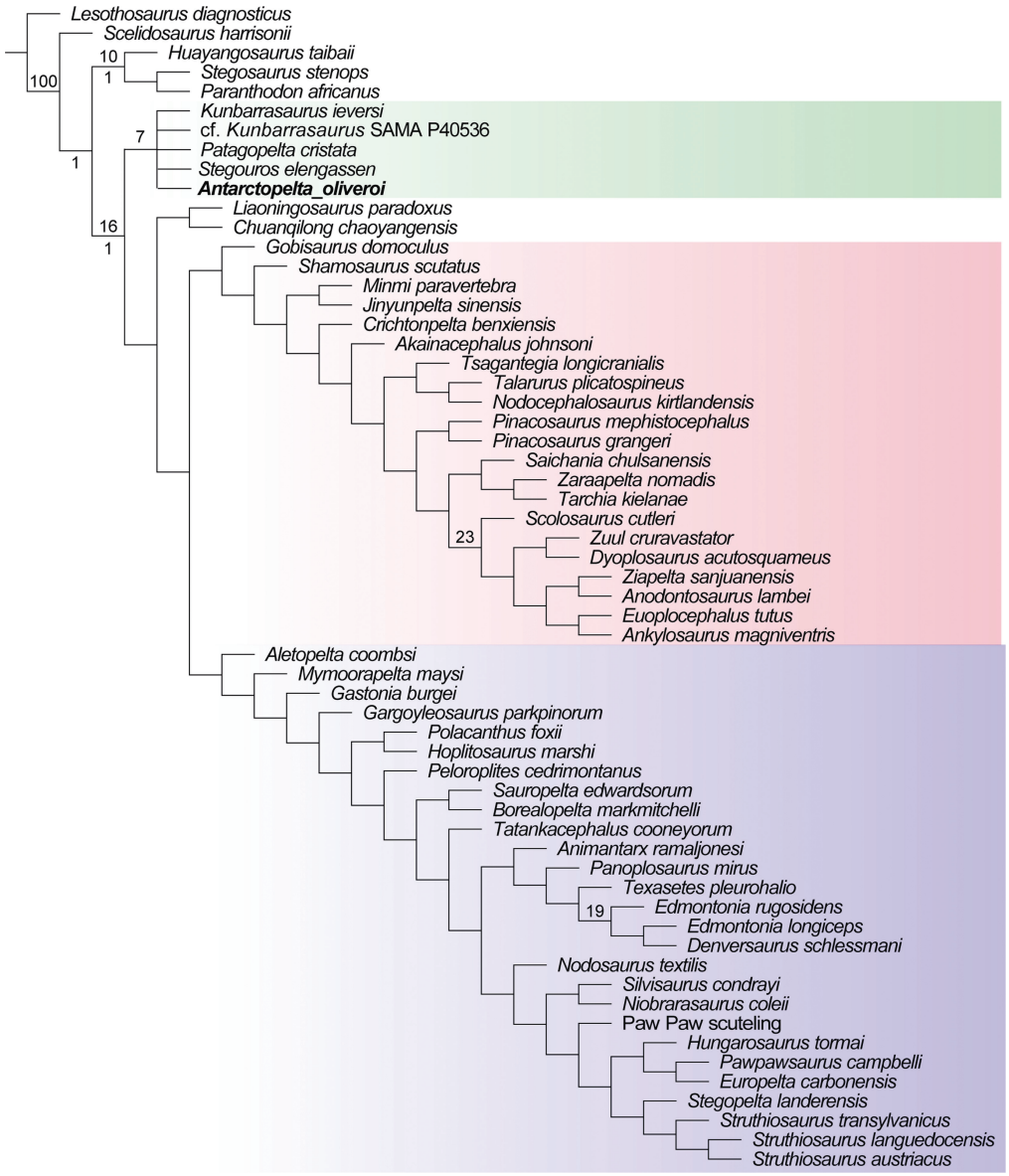

Figure 15 Result of the phylogenetic analysis of Ankylosauria. Reduced strict consensus of the 10000 MPTs of 704 steps (CI = 0.358, RI = 0.650, RC = 0.232) using a modified version of the matrix of Soto-Acuña et al. (2021), with the inclusion of cf. *Kunbarrasaurus* SAMA P40536, *Minmi paravertebra*, and adjustments of coding in *Patagopelta cristata* and *Antarctopelta oliveroi*. Parankylosauria is highlighted in green, Ankylosauridae in red and Nodosauridae in blue. Labels above the node are the bootstrap support values, while below the node is the Bremer support value.

Chinese early Cretaceous ankylosaurs (*Liaoningosaurus* + *Chuanqilong*) is recovered outside of Ankylosauridae + Nodosauridae. A similar result was obtained by Frauenfelder et al. (2022).

Minmi was found next to *Jinyunpelta*, at the base of Ankylosaurinae, however there is the possibility that it is an artifact due to the low percentage of coded characters in *Minmi*. Interestingly, the phylogenetic position of *Patagopelta*, which was probably recovered within Parankylosauria due to the changes made by us in the matrix, is in turn as a result of the direct observations and reinterpretation of the material published by Riguetti et al. (2022). A more detailed analysis of this question is outside the objective of this work, since new, more complete, and informative specimens would allow us to clarify this point (Agnolin et al., 2023).

7 Discussion

7.1 Taxonomical considerations and anatomical reinterpretation

Antarctopelta oliveroi has gone through a changing taxonomic history, beginning as an ankylosaurid, then a nodosaurid, later an ankylosaur of uncertain affinities and currently a parankylosaur. Even its taxonomical validity was put in question, arguing for a chimaera (Arbour and Currie, 2016). This uncertainty can be explained by: (1) the fragmentary nature of the only known specimen; and (2) the bizarre anatomy of the caudal vertebrae and the caudal osteoderms, which could only be reinterpreted with the discovery of new related ankylosaurs (Soto-Acuña et al., 2021). From the available material of the holotype, until now, the only cranial bone is the dentary. The rest of the alleged cranial bones turn out to be caudal osteoderms. The lack of more material and information about the excavation of the specimen, does not allow to propose a more heavily armored body. Moreover, the related *Stegouros elengassen* is characterized by the presence of few oval low-keeled osteoderms, as in *Antarctopelta*. Part of these osteoderms seem to be associated with the ribs, but more articulated specimens are needed to reconstruct the body armor and the epidermal structures. It is possible that *Antarctopelta* had several rows of paramedian osteoderms in the body. The presence of pieces of flat bones fused with fragment of ribs indicate the presence of dermal ossifications located in the sacral zone, as in *Stegouros*. On the other hand, the large, keeled, and concave osteoderms are almost identical to those of the caudal weapon of *Stegouros*. In addition, the few elements of the hindlimb shows a gracile extremity, as in an ankylosaur with light body armor, slender limbs, and a well-armed tail (Figure 16).

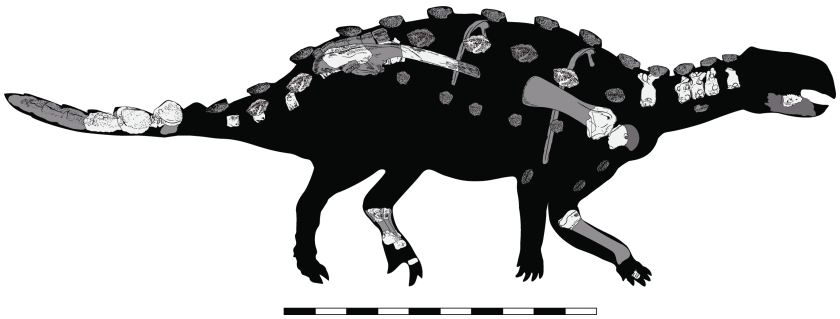

Figure 16 Skeletal reconstruction of *Antarctopelta oliveroi* based on the preserved elements of MLP-PV 86-X-28-1. The silhouette of this reconstruction was based on *Stegouros elengassen* (Soto-Acuña et al., 2021). Additional unpublished skeletal material of the same specimen has been discovered in the same locality (Coria et al., 2011) and in the collection of the MLP (Reguero pers. commun.), nevertheless, during the realization of this research, the material was under study for a thesis (Riguetti, 2023). Consequently, they were not included in this work. Scale bar = 100 cm.

Recently, new isolated specimens of ankylosaurs were reported from Antarctic Peninsula. These new descriptions include an isolated osteoderm (SDSM 142814) from the Maastrichtian Sandwich Bluff Member of the López de Bertodano Formation of Vega Island, referred to Nodosauridae? (Lamanna et al., 2019); and three osteoderms (CAV-A4, CAV-A5 and CAV-A10) from the Campanian–Maastrichtian Gamma Member of the Snow Hill Island, in James Ross Island (same geological unit from which comes MLP-PV 86-X-28-1), also referred to Nodosauridae (Brum et al., 2023). The current identification of isolated osteoderms in ankylosaurs, particularly nodosaurs and parankylosaurs is complex due to the lack of knowledge about the ontogenetic and interspecific variation, as to as the taxonomical validity of them. Brum et al. (2023) made a series of osteohistological sections to describe the histology of the osteoderms, based on the works of Burns and Currie (2014), which does not include parankylosaurs. On the other hand, they tested with a nonparametric Kruskal-Wallis tests, the morphology of these Antarctic osteoderms, however they excluded *Antarctopelta a priori* under the argument of an uncertain phylogenetic position, which is currently outdated (Frauenfelder et al., 2022; Riguetti et al., 2022; Soto-Acuña et al., 2021; Figure 15). Even if the morphology is compatible with nodosaur osteoderms, the alternatively hypothesis of parankylosaur

affinities cannot be discarded until taxa like of *Kunbarrasaurus* or *Stegouros* are histologically analyzed.

On the other hand, for the record from Sandwich Bluff Member of the López de Bertodano Formation, a parankylosaur affinity also cannot be rejected. Interestingly, the difference of the time deposition between the horizon of *Antarctopelta* and the presumed ankylosaur of López de Bertodano could indicate the persistence in time of the same taxon, or further, the existence of a new taxon at the very end of the Cretaceous. For the moment, in both cases the presence of a parankylosaur cannot be discarded.

7.2 Biogeographical implications

Beyond the current knowledge of the relationships of Gondwanan ankylosaurs, the hypothesis of a North American origin for South American and Antarctic ankylosaurs was the preferred scenario for decades (Coria and Salgado, 2001; Gasparini et al., 1996; Murray et al., 2019; Paulina-Carabajal et al., 2021; Salgado and Gasparini, 2006). The recognition of the early-diverging position of *Kunbarrasaurus* within Ankylosauria (then known as *Minmi* sp.) and some similarities with South American specimens led Agnolin et al. (2010) to propose the hypothesis of a wider distribution of Gondwanan ankylosaurs, instead of a dispersion event from North America. The phylogenetic analyses based on *Stegouros elengassen* and now in *Antarctopelta oliveroi* allowed to confirm this last idea, linking Australian, Antarctic, and South American ankylosaur of early diverging origin (Frauenfelder et al., 2022; Soto-Acuña et al., 2021). Recently a more complex scenario was proposed with the description of *Patagopelta cristata*, which was recovered as a nodosaur in a derived North American clade (Riguetti et al., 2022). However, iterations in the same matrices used before for *Stegouros* results in a parankylosaurian affinities for this taxon (Soto-Acuña et al., 2022), and more recently, new material from the Allen Formation (Campanian–Maastrichtian) seems to confirm this phylogenetic position (Agnolin et al., 2023) as well as in the analysis obtained here (Figure 15). Furthermore, a new and yet undescribed parankylosaur has been discovered in La Colonia Formation (Maastrichtian), Argentina (Becerra et al., 2023; Pol et al., 2023). This demonstrates that even if Parankylosauria were a rare component of the Campanian–Maastrichtian ecosystems, they were widely distributed in almost all of Patagonia (Figure 17).

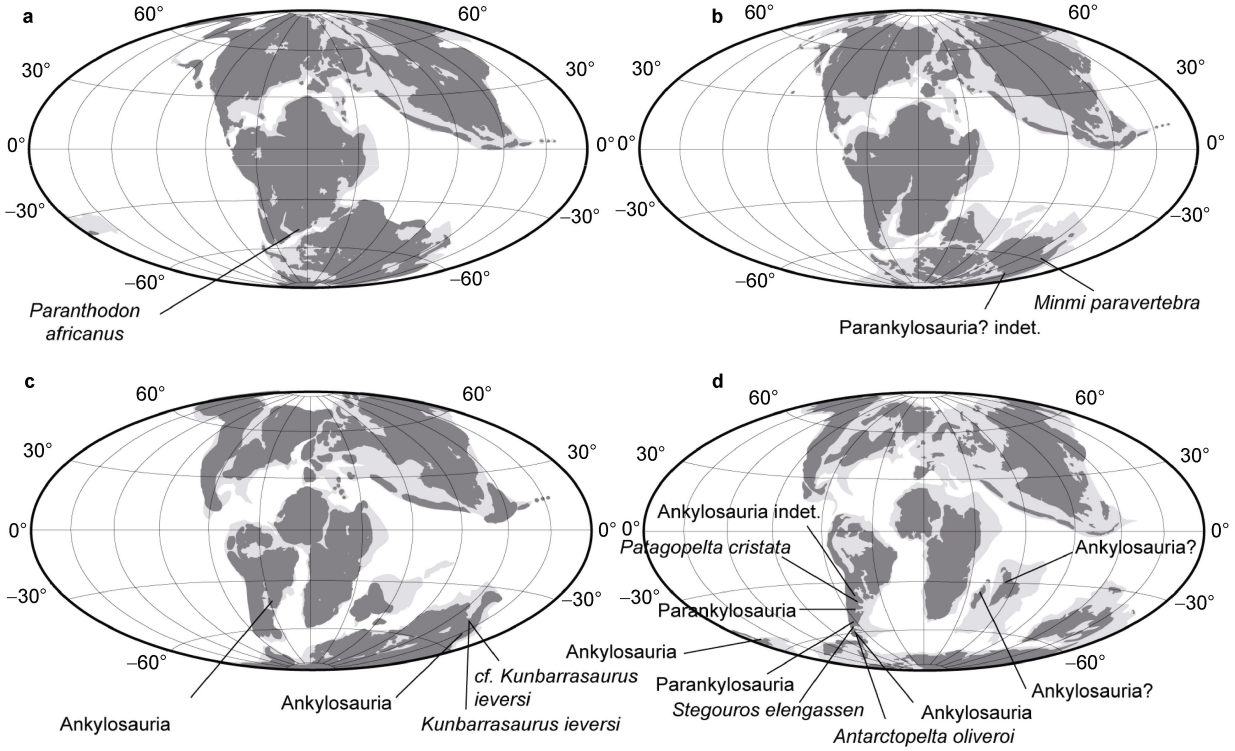

Figure 17 Distributions of Gondwanan findings of ankylosaurs during the Cretaceous. **a**, map of the world, during the Barremian–Aptian, with the fossil record of potential ankylosaurs in Gondwana; **b**, map of the world, during the Berriasian–Valanginian, with the fossil record of parankylosaurs of Gondwana; **c**, Albian–Cenomanian world with records of indeterminate ankylosaurs and parankylosaurs of Gondwana; **d**, Santonian–Maastrichtian world with fossil record of Parankylosauria. Note the high concentration of findings in South American Patagonia. Maps were redrawn from Scotese (2014a, 2014b). Data of the locations were based on Olivero et al. (1991); Gasparini et al., (2015); Leahey et al. (2015); Pereda-Suberbiola et al. (2015); Poropat et al. (2018); Raven and Maidment (2018); Soto-Acuña et al. (2021); Riguetti et al. (2022).

The absence of this clade in the fossil record before the Campanian in South America could be explained for different reasons. On of them is the obvious lack of more sampling in older units of Gondwanan landmasses (anthropogenic biases). Parankylosaurs diverge earlier, at least, during the Oxfordian (Soto-Acuña et al., 2021). During this lapse, the formation of the Caribbean corridor separates Laurasia from Gondwana (Iturralde-Vinent, 2006), and a few million years later, Gondwana began to fragment into two main continental masses, Western Gondwana (South America, Africa) and Eastern Gondwana (Madagascar, subcontinent India, Australia, Antarctica), and both of them progressively drifting away (Crisci et al., 1993; Énay et al., 1993; Scotese, 2001; 2014a). Until now, parankylosaurs are unknown in early Cretaceous deposits of Western Gondwana, but their presence in Australia from the Barremian is clear (Poropat et al., 2018). A conjunction of lack of systematic search, together with scarcity of rocks from this epoch could explain the apparent absence of Parankylosauria in Western Gondwana. Otherwise, parankylosaurs could be restricted to Eastern Gondwana during the early Cretaceous, arriving thereafter at South America through Western Antarctica during the late Cretaceous (Scotese, 2014b). The question remains, when did the Parankylosauria arrive to Patagonia? One possibility is that they never entered South America before the Campanian. The presence of *Antarctopelta oliveroi* in the Campanian–Maastrichtian of James Ross Island at least is consistent with this idea, however an alternative hypothesis of an earlier dispersion cannot be rejected. Notably, there are precedents for this second idea. During the Cenomanian–Turonian stages a great biotic turnover is recorded in the South American fossil record. Carcharodontosaurs, particularly Giganotosaurinae, together with the Rebachisauridae disappear from the fossil record (Canale et al., 2022; Salgado et al., 2022; Wilson and Allain, 2015). Otherwise, Megaraptoridae begins to be more present in this continent (Aranciaga-Rolando et al., 2022; Bell et al., 2016). The same biogeographical pattern is observed with Elasmaria (Bell et al, 2019; Duncan et al., 2021; Rozadilla et al., 2016) and the Unenlagiinae (Brum et al., 2021) whose pre-Cenomanian record is absent in South America as far as we known. Moreover, biogeographical analyses confirms that megaraptorids arrived at South America through Western Antarctica, from Australia (Bell et al., 2016), and a reverse event of dispersion occurred with the titanosaurs from the clade Diamantinasauria (Poropat et al., 2016). It is well known that a maximum thermal event (known as the KTM event) occurred during this lapse (Huber et al., 2018; Jarvis et al., 2011; Jones et al., 2022), which probably affected the latitudinal distribution of many species, allowing the existence of tropical forest near the South Pole (Klages et al., 2020). Could the parankylosaurs have dispersed from Australia to South America during this lapse? Only more complete material, together with systematic search in pre-Campanian rocks, could answer that question. For the moment, despite its fragmentary condition, *Antarctopelta oliveroi* is still a key taxon for their geographical location within the Biogeographic Weddellian Province.

8 Conclusions

The anatomy of almost complete specimens of related parankylosaurs, allows us reinterpret much of the anatomy of the holotype of *Antarctopelta oliveroi* (MLP-PV 86-X-28-1), which was considered for many years an enigmatic ankylosaur. Until now, *Antarctopelta* is the longest parankylosaur (around 4 m long) and is the only named ankylosaur in Antarctica. The presence of this taxon in the late Cretaceous of Antarctic Peninsula is consistent with a Weddellian Biogeographic distribution of Parankylosauria, the occurrence of which in late Cretaceous basins along Patagonia is just being unveiled. The presence of the Parankylosauria in South America is proposed as a dispersion event from Australia during the late Cretaceous.

Abbreviations

CAV-A: Centro Acadêmico de Vitória, Universidade Federal de Pernambuco, Pernambuco, Brazil.

CPAP: Colección de Paleontología de Antártica y Patagonia, Instituto Antártico Chileno, Punta Arenas, Chile.

IAA: Instituto Antártico Argentino, Dirección Nacional del Antártico, Argentina.

MPCA: Museo Provincial Carlos Ameghino, Cipolletti, Río Negro, Argentina.

MLP-PV: División Paleontología de Vertebrados, Museo de La Plata, Argentina.

MACN-PV: Museo Argentino de Ciencias Naturales Bernardino Rivadavia, Ciudad Autónoma de Buenos Aires, Argentina.

QM: Queensland Museum, Brisbane, Queensland, Australia.

SAMA: South Australian Museum, Adelaide, South Australia.

SDSM: South Dakota School of Mines and Technology, United States of America.

Acknowledgements We especially want to thank Marcelo Reguero (MLP), who gave us access to the holotype of *Antarctopelta oliveroi* in August 2019 and who also provided us with information and photographs of the find, giving us permission to use them. We also thank Yanina Herrera (MLP) for giving access again to the specimen for re-study in 2023. We appreciate the reviewers, Rodolfo Coria, Michael Burns, Leonardo Salgado, and Guest Editor (also Associate Editor) Dr. Javier Gelfo, for further improve the manuscripts. SSA was financed by PhD scholarship and by the “Beneficios de gastos operacionales 2023” both from ANID-Chile (Agencia Nacional de Investigación y Desarrollo, Chile). This research was supported by Núcleo Milenio EVOTEM from ANID-Gobierno de Chile.

References

Agnolin F L, Ezcurra M D, Pais D F, et al. 2010. A reappraisal of the Cretaceous non-avian dinosaur faunas from Australia and New

Zealand: evidence for their Gondwanan affinities. J Syst Palaeontol, 8(2): 257-300, doi:10.1080/14772011003594870.

Agnolin F L, Rozadilla S, Álvarez Nogueira R, et al. 2023. Nuevos restos del dinosaurio acorazado *Patagopelta cristata* Riguetti et al. (2022) y sus implicancias filogenéticas. La Rioja: XXXVI Jornadas Argentinas de Paleontología de Vertebrados.

Aranciaga Rolando A M, Motta M J, Agnolín F L, et al. 2022. A large Megaraptoridae (Theropoda: Coelurosauria) from upper cretaceous (maastrichtian) of Patagonia, Argentina. Sci Rep, 12: 6318, doi:10.1038/s41598-022-09272-z.

Arbour V M, Currie P J. 2013a. Euoplocephalus tutus and the diversity of ankylosaurid dinosaurs in the Late Cretaceous of Alberta, Canada, and Montana, USA. PLoS One, 8(5): e62421, doi:10.1371/journal.pone.0062421.

Arbour V M, Currie P J. 2013b. The taxonomic identity of a nearly complete ankylosaurid dinosaur skeleton from the Gobi Desert of Mongolia. Cretac Res, 46: 24-30, doi:10.1016/j.cretres.2013.08.008.

Arbour V M, Currie P J. 2016. Systematics, phylogeny and palaeobiogeography of the ankylosaurid dinosaurs. J Syst Palaeontol, 14(5): 385-444, doi:10.1080/14772019.2015.1059985.

Arbour V M, Mallon J C. 2017. Unusual cranial and postcranial anatomy in the archetypal ankylosaur *Ankylosaurus magniventris*. FACETS, 2(2): 764-794, doi:10.1139/facets-2017-0063.

Arbour V M, Zanno L E. 2018. The evolution of tail weaponization in amniotes. Proc Biol Sci, 285(1871): 20172299, doi:10.1098/rspb.2017.2299.

Arbour V M, Burns M E, Currie P J. 2011. A review of pelvic shield morphology in ankylosaurs (Dinosauria: Ornithischia). J Paleontol, 85(2): 298-302, doi:10.1666/10-071.1.

Arbour V M, Burns M E, Bell P R, et al. 2014. Epidermal and dermal integumentary structures of ankylosaurian dinosaurs. J Morphol, 275(1): 39-50, doi:10.1002/jmor.20194.

Arbour V M, Zanno L E, Gates T. 2016. Ankylosaurian dinosaur palaeoenvironmental associations were influenced by extirpation, sea-level fluctuation, and geodispersal. Palaeogeogr Palaeoclimatol Palaeoecol, 449: 289-299, doi:10.1016/j.palaeo.2016.02.033.

Barreda V D, Palamarczuk S, Medina F A. 1999. Palinología de la Formación Hidden Lake (Coniaciano-Santoniano), isla James Ross, Antártida. Revista Española de Micropaleontología, 31: 53-72.

Barrett P M, Rich T H, Vickers-Rich P, et al. 2010. Ankylosaurian dinosaur remains from the Lower Cretaceous of southeastern Australia. Alcheringa, 34(3): 205-217, doi:10.1080/03115511003655430.

Becerra M, Pol D, Carballido J L, et al. 2023. Parankylosaurian weaponry gets even stranger: new ankylosaur remains from the la Colonia Formation (Campanian-Maastrichtian) represent the most complete record in Argentina. Río Negro: Reunión de Comunicaciones de la Asociación Paleontológica Argentina 2023, 16-17.

Bell P R, Cau A, Fanti F, et al. 2016. A large-clawed theropod (Dinosauria: Tetanurae) from the Lower Cretaceous of Australia and the Gondwanan origin of megaraptorid theropods. Gondwana Res, 36: 473-487, doi:10.1016/j.gr.2015.08.004.

Bell P R, Burns M E, Smith E T. 2018. A probable ankylosaurian (Dinosauria, Thyreophora) from the Early Cretaceous of New South Wales, Australia. Alcheringa, 42(1): 120-124, doi:10.1080/03115518.2017.1384851.

Bell P R, Brougham T, Herne M C, et al. 2019. *Fostoria dhimbangunmal*, gen. et sp. nov., a new iguanodontian (Dinosauria, Ornithopoda) from the mid-Cretaceous of Lightning Ridge, New South Wales, Australia. J Vertebr Paleontol, 39(1): e1564757, doi:10.1080/02724634.2019.1564757.

Brown B. 1908. The Ankylosauridae, a new family of armored dinosaurs from the Upper Cretaceous. Bulletin of the AMNH, 24: 187-201.

Brum A S, Eleutério L H S, Simões T R, et al. 2023. Ankylosaurian body armor function and evolution with insights from osteohistology and morphometrics of new specimens from the Late Cretaceous of Antarctica. Paleobiology, 49(4): 579-600, doi:10.1017/pab.2023.4.

Brum A S, Pêgas R V, Bandeira K L N, et al. 2021. A new unenlagiine (Theropoda, Dromaeosauridae) from the Upper Cretaceous of Brazil. Pap Palaeontol, 7(4): 2075-2099, doi:10.1002/spp2.1375.

Bunzel E. 1871. Die Reptilfauna der Gosauformation in der Neuen Welt bei Weiner-Neustadt. Abhandlungen der Kaiserlich Königlichen Geologischen Reichsanstalt, 5: 1-18(in German).

Burns M E, Currie P J. 2014. External and internal structure of ankylosaur (Dinosauria, Ornithischia) osteoderms and their systematic relevance. J Vertebr Paleontol, 34(4): 835-851, doi:10.1080/02724634.2014.840309.

Canale J I, Apesteguía S, Gallina P A, et al. 2022. New giant carnivorous dinosaur reveals convergent evolutionary trends in theropod arm reduction. Curr Biol, 32(14): 3195-3202.e5, doi:10.1016/j.cub.2022.05.057.

Carpenter K. 2001. Phylogenetic analysis of the Ankylosauria//Carpenter K (ed). The armored dinosaurs. Bloomington: Indiana University Press, 455-483.

Carpenter K. 2004. Redescription of *Ankylosaurus magniventris* Brown 1908 (Ankylosauridae) from the Upper Cretaceous of the Western Interior of North America. Can J Earth Sci, 41(8): 961-986, doi:10.1139/e04-043.

Carpenter K, Miles C, Cloward K. 1998. Skull of a Jurassic ankylosaur (Dinosauria). Nature, 393: 782-783, doi:10.1038/31684.

Carpenter K, DiCroce T, Kinneer B, et al. 2013. Pelvis of *Gargoyleosaurus* (Dinosauria: Ankylosauria) and the origin and evolution of the ankylosaur pelvis. PLoS One, 8(11): e79887, doi:10.1371/journal.pone.0079887.

Cerda I A, Paulina Carabajal A, Salgado L, et al. 2012. The first record of a sauropod dinosaur from Antarctica. Naturwissenschaften, 99(1): 83-87, doi:10.1007/s00114-011-0869-x.

Cerda I A, Gasparini Z, Coria R A, et al. 2019. Paleobiological inferences for the Antarctic dinosaur Antarctopelta oliveroi (Ornithischia: Ankylosauria) based on bone histology of the holotype. Cretac Res, 103: 104171, doi:10.1016/j.cretres.2019.07.001.

Chatterjee S, Rudra D K. 1996. KT events in India: impact, rifting, volcanism and dinosaur extinction. Mem Que Mus, 39(3): 489-532.

Coombs W P Jr. 1978. The families of the ornithischian dinosaur Order Ankylosauria (Reptilia: Ornithischia). Palaeontology, 21: 143-170.

Coombs W P Jr, Maryanska T. 1990. Ankylosauria//Weishampel D B, Dodson P, Osmolska H (eds). The dinosauria. Berkeley: University of California Press, 456-483.

Coria R A, Salgado L. 2001. South American ankylosaurs//Carpenter K (ed). The armored dinosaurs. Bloomington: Indiana University Press, 159-168.

Coria R A, Salgado L, Gasparini Z, et al. 2011. Nuevos materiales del ejemplar holotipo de *Antarctopelta oliveroi* Salgado y Gasparini (Dinosauria, Ornithischia, Ankylosauria) del Cretácico superior de Antártida.Reunión Asociación Paleontológica Argentina, 2011. Ameghiniana, 48(4): R10.

Coria R A, Moly J J, Reguero M, et al. 2013. A new ornithopod

(Dinosauria; Ornithischia) from Antarctica. Cretac Res, 41: 186-193, doi:10.1016/j.cretres.2012.12.004.

Crame J A, Pirrie D, Riding J B, et al. 1991. Campanian–Maastrichtian (Cretaceous) stratigraphy of the James ross island area, Antarctica. J Geol Soc, 148(6): 1125-1140, doi:10.1144/gsjgs.148.6.1125.

Crame J A, Pirrie D, Riding J B. 2006. Mid-cretaceous stratigraphy of the James ross Basin, Antarctica. Geol Soc Lond Spec Publ, 258(1): 7-19, doi:10.1144/gsl.sp.2006.258.01.02.

Crisci J V, de la Fuente M S, Lanteri A A, et al. 1993. Patagonia, Gondwana Occidental (GW) y Oriental (GE), un modelo de biogeografía histórica. Ameghiniana, 30, 104.

De Valais S, Apesteguía S, Udrizar Sauthier D. 2003. Nuevas evidencias de dinosaurios de la Formación Puerto Yeruá (Cretácico), Provincia de Entre Ríos, Argentina. Ameghiniana, 40(3): 507-502.

del Valle R A, Elliot D H, MacDonald D I M. 1992. Sedimentary basins on the east flank of the Antarctic Peninsula: proposed nomenclature. Antarct Sci, 4(4): 477-478, doi:10.1017/S0954102092000695.

Duncan R J, Evans A R, Vickers-Rich P, et al. 2021. Ornithopod jaws from the Lower Cretaceous Eumeralla Formation, Victoria, Australia, and their implications for polar neornithischian dinosaur diversity. J Vertebr Paleontol, 41(3): e1946551, doi:10.1080/02724634.2021.1946551.

Eaton T H J. 1960. A new armored dinosaur from the Cretaceous of Kansas. Lawrence: The University of Kansas Press, 8: 1-24.

Énay R, Cariou E, Mangold C, et al. 1993. Callovian (162-158 Ma)// Dercourt J, Ricou L E, Vrielynck B (eds). Atlas Tethys paleoenvironmental maps, Rueil-Malmaison: Beicip-Franlab.

Estes R, De Queiroz K, Gauthier J. 1988. Phylogenetic relationships within Squamata//Estes R, Pregill G (eds). Phylogenetic relationships of the lizard families: essays commemorating Charles L. Camp. Stanford: Stanford University Press, 119-281.

Frauenfelder T G, Bell P R, Brougham T, et al. 2022. New ankylosaurian cranial remains from the Lower Cretaceous (Upper Albian) Toolebuc Formation of Queensland, Australia. Front Earth Sci, 10: 803505, doi:10.3389/feart.2022.803505.

Galton P M. 1980. Partial skeleton of *Dracopelta zbyszewskii* n. gen. and n. sp., an ankylosaurian dinosaur from the Upper Jurassic of Portugal. Geobios, 13(3): 451-457, doi:10.1016/s0016-6995(80)80081-7.

Galton P M. 2019. Earliest record of an ankylosaurian dinosaur (Ornithischia: Thyreophora): Dermal armor from Lower Kota Formation (Lower Jurassic) of India. Njgpa, 291(2): 205-219, doi:10.1127/njgpa/2019/0800.

Galton P M, Upchurch P. 2004. Stegosauria//Weishampel D B, Dodson P, Osmólska H (eds). The Dinosauria (2nd edition). Berkeley: University of California Press, 343-362.

Gasparini Z, Olivero E, Scasso R, et al. 1987. Un ankilosaurio (Reptilia, Ornithischia) Campaniano en el continente antártico. Río de Janeiro: Anais do X Congresso Brasileiro de Paleontologia, 131-141.

Gasparini Z, Pereda-Suberbiola X, Molnar R E. 1996. New data on the ankylosaurian dinosaur from the Late Cretaceous of the Antarctic Peninsula. Mem Que Mus, 39(3): 583-594.

Gasparini Z, Sterli J, Parras A, et al. 2015. Late Cretaceous reptilian biota of the La Colonia Formation, central Patagonia, Argentina: occurrences, preservation and paleoenvironments. Cretac Res, 54: 154-168, doi:10.1016/j.cretres.2014.11.010.

Gilmore C W. 1930. On dinosaurian reptiles from the Two Medicine Formation of Montana. Proc U S Natl Mus, 77(2839): 1-39, 18figs., 10pls., doi:10.5479/si.00963801.77-2839.1.

Goloboff P A, Catalano S A. 2016. TNT version 1.5, including a full implementation of phylogenetic morphometrics. Cladistics, 32(3): 221-238, doi:10.1111/cla.12160.

Han F L, Zheng W J, Hu D Y, et al. 2014. A new basal ankylosaurid (Dinosauria: Ornithischia) from the Lower Cretaceous Jiufotang Formation of Liaoning Province, China. PLoS One, 9(8): e104551, doi:10.1371/journal.pone.0104551.

Hendrickx C, Mateus O, Araújo R. 2015. A proposed terminology of theropod teeth (Dinosauria, Saurischia). J Vertebr Paleontol, 35(5): e982797, doi:10.1080/02724634.2015.982797.

Huber B T, MacLeod K G, Watkins D K, et al. 2018. The rise and fall of the Cretaceous Hot Greenhouse climate. Glob Planet Change,167: 1-23, doi:10.1016/j.gloplacha.2018.04.004.

Iturralde-Vinent M A. 2006. Meso-cenozoic Caribbean paleogeography: implications for the historical biogeography of the region. Int Geol Rev, 48(9): 791-827,

Jarvis I, Lignum J S, Gröcke D R, et al. 2011. Black shale deposition, atmospheric CO_2 drawdown, and cooling during the Cenomanian-Turonian Oceanic Anoxic Event. Paleoceanography, 26(3): PA3201, doi:10.1029/2010pa002081.

Jones M M, Petersen S V, Curley A N. 2022. A tropically hot mid-Cretaceous North American Western Interior Seaway. Geology, 50(8): 954-958, doi:10.1130/G49998.1.

Jordan T A, Riley T R, Siddoway C S. 2020. The geological history and evolution of West Antarctica. Nat Rev Earth Environ, 1: 117-133, doi:10.1038/s43017-019-0013-6.

Kennedy W J, Crame J A, Bengtson P, et al. 2007. Coniacian ammonites from James Ross Island, Antarctica. Cretac Res, 28(3): 509-531, doi:10.1016/j.cretres.2006.08.006.

Kirkland J I, Carpenter K. 1994. North America's first pre-Cretaceous ankylosaur (Dinosauria) from the Upper Jurassic Morrison Formation of western Colorado. BYU Geol Stud, 40: 25-42.

Kirkland J I, Alcalá L, Loewen M A, et al. 2013. The basal nodosaurid ankylosaur *Europelta carbonensis* n. gen., n. sp. from the Lower Cretaceous (Lower Albian) escucha formation of northeastern Spain. PLoS One, 8(12): e80405, doi:10.1371/journal.pone.0080405.

Klages J P, Salzmann U, Bickert T, et al. 2020. Temperate rainforests near the South Pole during peak Cretaceous warmth. Nature, 580(7801): 81-86, doi:10.1038/s41586-020-2148-5.

Lamanna M C, Case J A, Roberts E M, et al. 2019. Late Cretaceous non-avian dinosaurs from the James Ross Basin, Antarctica: description of new material, updated synthesis, biostratigraphy, and paleobiogeography. Adv Polar Sci, 30(3): 228-250, doi:10.13679/j.advps.2019.0007.

Lambe L M. 1902. New genera and species from the Belly River Series (mid-Cretaceous). Geological Survey of Canada Contributions to Canadian Palaeontology, 3: 25-81, doi:10.5281/zenodo.3233762.

Lambe L M. 1919. Description of a new genus and species (*Panoplosaurus mirus*) of an armoured dinosaur from the Belly River Beds of Alberta. Toronto: Transactions of the Royal Society of Canada, 13, 39-50.

Leahey L G, Salisbury S W. 2013. First evidence of ankylosaurian dinosaurs (Ornithischia: Thyreophora) from the mid-Cretaceous (late Albian–Cenomanian) Winton Formation of Queensland, Australia. Alcheringa, 37(2): 249-257, doi:10.1080/03115518.2013.743703.

Leahey L G, Molnar R E, Carpenter K, et al. 2015. Cranial osteology of the ankylosaurian dinosaur formerly known as *Minmi* sp. (Ornithischia: Thyreophora) from the Lower Cretaceous Allaru Mudstone of Richmond, Queensland, Australia. PeerJ, 3: e1475, doi:10.7717/peerj.1475.

Leahey, L. G., Molnar, R. E. and Salisbury, S. W. (2019). More than *Minmi*: a new Australian ankylosaurian dinosaur from the Lower Cretaceous (Albian) of Queensland, with implications for understanding global thyreophoran diversity. Brisbane: 79th Annual Meeting of the Society of Vertebrate Paleontology, 139.

Lee Y N. 1996. A new nodosaurid ankylosaur (Dinosauria: Ornithischia) from the Paw Paw Formation (Late Albian) of Texas. J Vertebr Paleontol, 16(2): 232-245, doi:10.1080/02724634.1996.10011311.

Lydekker R. 1893. On the jaw of a new carnivorous dinosaur from the Oxford Clay of Peterborough. Q J Geol Soc, 49(1-4): 284-287, doi:10.1144/gsl.jgs.1893.049.01-04.46.

Macdonald D I M, Barker P F, Garrett S W, et al. 1988. A preliminary assessment of the hydrocarbon potential of the Larsen Basin, Antarctica. Mar Pet Geol, 5(1)：34-53, doi:10.1016/0264-8172(88)90038-4.

Maleev E A. 1955. Armored dinosaurs of the Upper Cretaceous of Mongolia, family Ankylosauridae. Trudy Palaeontologicheskoi Instytuta, Akademiia Nauk SSSR 62: 51-91 (in Russian, translation by Welch R).

Maddison W P, Maddison D R. 2019. Mesquite: a modular system for evolutionary analysis. http://www.mesquiteproject.org.

Maidment S C R, Raven T J, Ouarhache D, et al. 2020. North Africa's first stegosaur: implications for Gondwanan thyreophoran dinosaur diversity. Gondwana Res, 77: 82-97, doi:10.1016/j.gr.2019.07.007.

Maidment S C R, Strachan S J, Ouarhache D, et al. 2021. Bizarre dermal armour suggests the first African ankylosaur. Nat Ecol Evol, 5(12): 1576-1581, doi:10.1038/s41559-021-01553-6.

Armored dinosaurs of the Upper Cretaceous of Mongolia. Acad Sci USSR, 104(5): 779-783 (in Russian, translation by Alcock F J).

Mantell G. 1833. The geology of the South-East of England. London: Longman.

Maryanska T. 1977. Ankylosauridae (Dinosauria) from Mongolia. Palaeontologia Polonica, 37: 85-151.

McArthur J M, Crame J A, Thirlwall M F. 2000. Definition of Late Cretaceous stage boundaries in Antarctica using strontium isotope stratigraphy. J Geol, 108(6): 623-640, doi:10.1086/317952.

Milanese F N, Olivero E B, Kirschvink J L, et al. 2017. Magnetostratigraphy of the Rabot Formation, Upper Cretaceous, James Ross Basin, Antarctic Peninsula. Cretac Res, 72: 172-187, doi:10.1016/j.cretres.2016.12.016.

Milanese F N, Olivero E B, Raffi M E, et al. 2019. Mid Campanian-Lower Maastrichtian magnetostratigraphy of the James Ross Basin, Antarctica: Chronostratigraphical implications. Basin Res, 31(3): 562-583, doi:10.1111/bre.12334.

Milanese F N, Olivero E B, Slotznick S P, et al. 2020. Coniacian–Campanian magnetostratigraphy of the Marambio Group: the Santonian–Campanian boundary in the Antarctic Peninsula and the complete Upper Cretaceous–Lowermost Paleogene chronostratigraphical framework for the James Ross Basin. Palaeogeogr Palaeoclimatol Palaeoecol, 555, doi:10.1016/j.palaeo.2020.109871.

Molnar R E. 1980. An ankylosaur (Ornithischia: Reptilia) from the Lower Cretaceous of southern Queensland. Mem Que Mus, 20(1): 77-87.

Molnar R E. 1996. Preliminary report on a new ankylosaur from the Early Cretaceous of Queensland, Australia. Mem Que Mus, 39(3): 653-668.

Molnar R E. 2001. Armor of the small ankylosaur *Minmi*//Carpenter K (ed). The armored dinosaurs. Bloomington: Indiana University Press, 341-362.

Molnar R E, Wiffen J. 1994. A Late Cretaceous polar dinosaur fauna from New Zealand. Cretac Res, 15(6): 689-706, doi:10.1006/cres.1994.1038.

Murray A, Riguetti F, Rozadilla S. 2019. New ankylosaur (Thyreophora, ornithischia) remains from the Upper Cretaceous of Patagonia. J S Am N Earth Sci, 96: 102320, doi:10.1016/j.jsames.2019.102320.

Nopcsa F. 1915. Die Dinosaurier der Siebenbürgischen Landesteile Ungarns. Mitteilungen aus dem Jahrbuch der königlichen Ungarischen Geologischen Reichsanstalt Budapest, 23(1): 1-24.

Nopcsa F. 1928. Palaeontological notes on reptiles. Budapestini: Sumptibus Instituti Regni Hungariae Geologic, 1-84.

Olivero E B. 2012a. Sedimentary cycles, ammonite diversity and palaeoenvironmental changes in the Upper Cretaceous Marambio Group, Antarctica. Cretac Res, 34: 348-366, doi:10.1016/j.cretres.2011.11.015.

Olivero E B. 2012b. New Campanian kossmaticeratid ammonites from the James Ross Basin, Antarctica, and their possible relationships with *Jimboiceras*? *antarcticum* Riccardi. Revue de Paléobiologie, Genève, 11: 133-149.

Olivero E, Gasparini Z, Rinaldi, C. and Scasso R. (1991). First record of dinosaurs in Antarctica (Upper Cretaceous, James Ross Island): paleogeographical implications//Thomson M R A, Crame J A, Thomson J W (eds). Geological evolution of Antarctica. Cambridge: Cambridge University Press, 617-622.

Ősi A. 2005. *Hungarosaurus tormai*, a new ankylosaur (Dinosauria) from the Upper Cretaceous of Hungary. J Vertebr Paleontol, 25(2): 370-383, doi:10.1671/0272-4634(2005)025[0370: htanad]2.0.co;2.

Ostrom J H. 1970. Stratigraphy and paleontology of the Cloverly Formation (Lower Cretaceous) of the Bighorn Basin area, Wyoming and Montana. New Haven: Peabody Museum of Natural History.

O'Gorman J P. 2020. Elasmosaurid phylogeny and paleobiogeography, with a reappraisal of *Aphrosaurus furlongi* from the Maastrichtian of the Moreno Formation. J Vertebr Paleontol, 39(5): e1692025, doi:10.1080/02724634.2019.1692025.

Parks W A. 1924. *Dyoplosaurus acutosquameus*, a new genus and species of armored dinosaur, and notes on a skeleton of *Prosaurolophus maximus*. Tronto: University of Toronto Studies, 18: 1-35.

Paulina-Carabajal A, Barrios F T, Méndez A H, et al. 2021. A Late Cretaceous dinosaur and crocodyliform faunal association-based on isolate teeth and osteoderms-at Cerro Fortaleza Formation (Campanian-Maastrichtian) type locality, Santa Cruz, Argentina. PLoS One, 16(9): e0256233, doi:10.1371/journal.pone.0256233.

Penkalski P. 2001. Variation in specimens referred to *Euoplocephalus tutus*//Carpenter K (ed). The armored dinosaurs. Bloomington: Indiana University Press, 363-385.

Penkalski P. 2013. A new ankylosaurid from the Late Cretaceous Two Medicine Formation of Montana, USA. Acta Palaeontol Pol, 59(3): 617-634, doi:10.4202/app.2012.0125.

Penkalski P. 2018. Revised systematics of the armoured dinosaur *Euoplocephalus* and its allies. N Jb Geol Paläont Abh, 287(3): 261-306, doi:10.1127/njgpa/2018/0717.

Pereda-Suberbiola X, Díaz-Martínez I, Salgado L, et al. 2015. Síntesis del registro fósil de dinosaurios tireóforos en Gondwana. Publicación Electrónica de la Asociación Paleontológica Argent: 90-107, doi:10.5710/peapa.21.07.2015.101 (in Spanish with English abstract).

Piveteau J. 1926. Contribution à l'étude des formations lagunaires du Nord-Ouest de Madagascar. Bulletin de la Societé Géologique de France, 5(26): 33-38.

Pol D, Becerra M, Carballido J L, et al. 2023. New dinosaur discoveries in the la Colonia Formation: insights into the late Cretaceous fauna of

Patagonia before the K-Pg extinction event. Cincinnati, Ohio: 83rd Annual Meeting of the Society of Vertebrate Paleontology, 530.

Pol D, Escapa I H. 2009. Unstable taxa in cladistic analysis: identification and the assessment of relevant characters. Cladistics, 25(5): 515-527, doi:10.1111/j.1096-0031.2009.00258.x.

Poropat S F, Martin S K, Tosolini A M P, et al. 2018. Early Cretaceous polar biotas of Victoria, southeastern Australia—an overview of research to date. Alcheringa, 42(2): 157-229, doi:10.1080/03115518. 2018.1453085.

Poropat S F, Mannion P D, Upchurch P, et al. 2016. New Australian sauropods shed light on Cretaceous dinosaur palaeobiogeography. Sci Rep, 6: 34467, doi:10.1038/srep34467.

Raven T J, Barrett P M, Pond S B, et al. 2020. Osteology and taxonomy of British Wealden Supergroup (Berriasian–Aptian) ankylosaurs (Ornithischia, Ankylosauria). J Vertebr Paleontol, 40(4): e1826956, doi:10.1080/02724634.2020.1826956.

Raven T J, Barrett P M, Joyce C B, et al. 2023. The phylogenetic relationships and evolutionary history of the armoured dinosaurs (Ornithischia: Thyreophora). J Syst Palaeontol, 21(1): 2205433, doi:10.1080/14772019.2023.2205433.

Raven T J, Maidment S C R. 2018. The systematic position of the enigmatic thyreophoran dinosaur *Paranthodon africanus*, and the use of basal exemplifiers in phylogenetic analysis. PeerJ, 6: e4529, doi: 10.7717/peerj.4529.

Reguero M A, Goin F J. 2021. Paleogeography and biogeography of the Gondwanan final breakup and its terrestrial vertebrates: new insights from southern South America and the "double Noah's Ark" Antarctic Peninsula. J S Am N Earth Sci, 108: 103358, doi:10.1016/j.jsames. 2021.103358.

Reguero M A, Gasparini Z, Olivero E B, et al. 2022. Late Campanian–early Maastrichtian vertebrates from the James Ross Basin, West Antarctica: updated synthesis, biostratigraphy, and paleobiogeography. An Acad Bras Cienc, 94(suppl 1): e20211142, doi:10.1590/0001-3765202220211142.

Reguero M A, Tambussi C P, Coria R A, et al. 2013. Late cretaceous dinosaurs from the James Ross Basin, West Antarctica. Geol Soc Lond Spec Publ, 381(1): 99-116, doi:10.1144/sp381.20.

Riguetti F. 2023. Thyreophora en Gondwana: revisión del clado con énfasis en Sudamérica, búsqueda y análisis de nuevos restos del Cretácico sudamericano. Buenos Aires: Universidad de Buenos Aires, 332.

Riguetti F, Pereda-Suberbiola X, Ponce D, et al. 2022. A new small-bodied ankylosaurian dinosaur from the Upper Cretaceous of North Patagonia (Río Negro Province, Argentina). J Syst Palaeontol, 20(1): 2137441, doi:10.1080/14772019.2022.2137441.

Roberts E M, Lamanna M C, Clarke J C, et al. 2014. Stratigraphy and vertebrate paleoecology of Upper Cretaceous–?lowest Paleogene strata on Vega Island, Antarctica. Palaeogeogr Palaeoclimatol Palaeoecol, 402: 55-72, doi:10.1016/j.palaeo.2014.03.005.

Rozadilla S, Agnolin F L, Novas F E, et al. 2016. A new ornithopod (Dinosauria, Ornithischia) from the Upper Cretaceous of Antarctica and its palaeobiogeographical implications. Cretac Res, 57: 311-324, doi:10.1016/j.cretres.2015.09.009.

Rozadilla S, Agnolín F, Manabe M, et al. 2021. Ornithischian remains from the Chorrillo Formation (Upper Cretaceous), southern Patagonia, Argentina, and their implications on ornithischian paleobiogeography in the Southern Hemisphere. Cretac Res, 125: 104881, doi:10.1016/j. cretres.2021.104881.

Salgado L, Coria R A. 1996. First evidence of an ankylosaur (Dinosauria, Ornithischia) in South America. Ameghiniana, 33(4): 367-371.

Salgado L, Gasparini Z. 2006. Reappraisal of an ankylosaurian dinosaur from the Upper Cretaceous of James Ross Island (Antarctica). Geodiversitas, 28(1): 119-135.

Salgado L, Gallina P A, Lerzo L N, et al. 2022. Highly specialized diplodocoids: the Rebbachisauridae//Otero A, Carballido J L, Pol D (eds). South American sauropodomorph dinosaurs. Cham: Springer, 165-208, doi:10.1007/978-3-030-95959-3_5.

Scheyer T M, Sander P M. 2004. Histology of ankylosaur osteoderms: implications for systematics and function. J Vertebr Paleontol, 24(4): 874-893, doi:10.1671/0272-4634(2004)024[0874: hoaoif]2.0.co;2.

Scotese C R. 2001. Atlas of earth history. Arlington: PALEOMAP Project. http://scotese.com.

Scotese C R. 2014a. Atlas of Early Cretaceous Paleogeographic maps, PALEOMAP Atlas for ArcGIS, volume 2, The Cretaceous, maps 23-31, Mollweide Projection, PALEOMAP Project, Evanston, IL.

Scotese C R. 2014b. Atlas of Late Cretaceous Maps, PALEOMAP Atlas for ArcGIS, volume 2, The Cretaceous, Maps 16-22, Mollweide Projection. Evanston: PALEOMAP Project.

Sereno P C. 1986. Phylogeny of the bird-hipped dinosaurs (Order Ornithischia). Natl Geogr Res, 2: 234-256.

Soto-Acuña S, Vargas A O, Kaluza J, et al. 2021. Bizarre tail weaponry in a transitional ankylosaur from subantarctic Chile. Nature, 600(7888): 259-263, doi:10.1038/s41586-021-04147-1.

Soto-Acuña S, Vargas A O, Alarcón-Muñoz, et al. 2022. Relaciones filogenéticas de los anquilosaurios (Ornithischia: Ankylosauria) del Cretácico de Gondwana. Tagua: II Congreso Chileno de Paleontología, San Vicente de Tagua, 116.

Thompson R S, Parish J C, Maidment S C R, et al. 2012. Phylogeny of the ankylosaurian dinosaurs (Ornithischia: Thyreophora). J Syst Palaeontol, 10(2): 301-312, doi:10.1080/14772019.2011.569091.

Tumanova T A. 1983. The first ankylosaur from the Lower Cretaceous of Mongolia. Trans Sov Mong Exp, 24: 110-120 (translation by Welch R).

Vickaryous M, Maryańska T, Weishampel D. 2004. Ankylosauria// Weishampel D B, Dodson P, Osmólska (eds). The Dinosauria, second edition. Berkeley: University of California Press, 363-392.

Xu X, Wang X L, You H L. 2001. A juvenile ankylosaur from China. Naturwissenschaften, 88(7): 297-300, doi:10.1007/s001140100233.

Yang J T, You H L, Li D Q, et al. 2013. First discovery of polacanthine ankylosaur dinosaur in Asia. Vertebrata Palasiatica, 51(4): 265-277, doi:10.19615/j.cnki.1000-3118.2013.04.002 (in Chinese with English abstract).

Welles S P. 1952. A review of the North American Cretaceous elasmosaurs. Berkeley: University of California Press, 47-143.

Wilson J A, Allain R. 2015. Osteology of *Rebbachisaurus garasbae* Lavocat, 1954, a diplodocoid (Dinosauria, Sauropoda) from the early Late Cretaceous–aged Kem Kem beds of southeastern Morocco. J Vertebr Paleontol, 35(4): e1000701, doi:10.1080/02724634.2014. 1000701.

Witts J D, Whittle R J, Wignall P B, et al. 2016. Macrofossil evidence for a rapid and severe Cretaceous–Paleogene mass extinction in Antarctica. Nat Commun, 7: 11738, doi:10.1038/ncomms11738.

Zheng W J, Jin X S, Azuma Y, et al. 2018. The most basal ankylosaurine dinosaur from the Albian–Cenomanian of China, with implications for the evolution of the tail club. Sci Rep, 8(1): 3711, doi:10.1038/ s41598-018-21924-7.

Supplementary Table, Text and Matrix

Table S1 Measurements of selected bones, from *Antarctopelta oliveroi* MLP-PV 86-X-28-1. In asterisk the measurements inferred from partially preserved and mirrorable elements are shown

	Length/mm	Width/mm	Height/mm
Distance between meckelian canal and occlusal surface at the level of the fourth preserved alveolus	–	–	36.11
Crown of the best-preserved tooth	5.09	3.51	5.63
Anterior cervical centrum	42.02	49.25	38.70
Posterior cervical centrum	46.92	61.50	56.78
1st dorsosacral centrum	56.08	69.93	39.02
1st sacral centrum	56.39	71.47	31.17
Anterior caudal centrum	40.52	62.91*	45.54
Posterior caudal centrum	56.97	50.34	34.49
Transverse process of posterior caudal vertebra	44.08	–	5.21
Coracoid contribution to glenoid	50.31	–	–
Scapular contribution to glenoid	70.27	–	–
Manual phalanx	31.69	29.48	39.09
Distal epiphysis radius	–	57.15	–
Preacetabular fragment	–	–	31.87
Distal epiphysis Metacarpal II	–	41.06	43.82
Proximal epiphysis Metacarpal III	–	37.53	52.51
Distal epiphysis Metacarpal III	–	52.53	43.56
Proximal epiphysis Metacarpal IV	–	57.10	50.40
Distal epiphysis Metacarpal IV	–	47.79	49.25
Free keeled osteoderm	75.68	46.01	37.78
Caudal dorsal plate	76.61	116.35	37.25
Caudal ventral plate	58.78	54.29	66.47

Note: * indicates a measurement estimated by mirroring the preserved portion.

Text S1 Changes in phylogenetic matrix

The chosen matrix was that of Arbor and Currie (2016), modified by Soto-Acuña et al. (2021), which in addition to incorporating changes in the coding of some taxa, adds new information from several euripods (*Akainacephalus*, cf. *Kunbarrasaurus*, *Borealopelta*, *Jinyunpelta*, *Minmi Paranthodon*, *Stegouros*, *Talarurus*, *Zuul*), resulting in a 189×65 matrix. In this work, the following characters were incorporated:

Char. 190. Choanae with their anterior margins inline or within the anterior third of the maxillary tooth row (0); choanae posteriorly situated with their anterior margins at least mid-way along the tooth row (1). Taken from Frauenfelder et al. (2022).

Char. 191. Coracoid/scapula length ratio: coracoid less than half the scapula length (0), more than half (1). Taken from Riguetti et al. (2022).

Additionally, changes were made in the states of some characters in the following taxa based on direct observation and the work of Raven et al. (2020).

Hylaeosaurus armatus

Char. 46. Squamosal/postorbital horn: no horn (0) base has broad triangular cross-section and overall shape is pyramidal (1), base is oval in cross-section and overall shape is narrow, tapered cylinder (2). Changed from 1 to ?.

Char. 95. Dimensions of cervical vertebrae centra: anteroposteriorly longer than transverse width (0), anteroposteriorly shorter than transverse width (1). Changed from 1 to 0.

Char. 97. Ratio of anteroposterior dorsal centrum length to posterior centrum height: >1.1 (0), <1.1 (1). Changed from ? to 0.

Char. 98 Longitudinal keel on ventral surface of dorsal centra: present (0), absent (1). Changed from 0 to [0 1].

Char. 99. Cross sectional shape of neural canal in posterior dorsals: circular (0) elliptical, with long axis running dorsoventrally (1). Changed from 0 to 1.

Char. 100. Shape of the proximal cross-section of the dorsal ribs: triangular (0), "L"- or "T"-shaped (1). Changed from ? to 1.

Char. 106. Direction of the transverse processes of proximal caudals: craniolaterally projecting (0), caudolaterally projecting (1), laterally projecting (2). Changed from 0 to ?.

Char. 107. Persistence of transverse processes down the length of the caudal series: not present beyond the mid-length of the series (0), present beyond the mid-length of the series (1). Changed from 1 to ?.

Char. 108. Attachment of haemal arches to their respective centra: articulated (0), fused (1). Changed from 0 to ?.

Char. 109. Extent of pre- and postzygapophyses over their adjacent centra in posterior vertebrae: extend over less than half the length of the adjacent centrum (0), extend over more than half the length of the adjacent centrum (1). Changed from 0 to ?.

Char. 110. In tail club handle vertebrae, shape of each interlocking neural arch in dorsal view: distal caudal vertebrae do not form handle (0), V-shaped, angle of divergence about 22°–26° (1), V-shaped, angle of divergence about 35°–37° (2), U-shaped, angle of divergence greater than 60° (3). Changed from 0 to ?.

Char. 111. Shape of the posterior haemal arches: rounded haemal spine in lateral view with no contact between haemal arches (0), inverted "T"-shaped haemal spine in lateral view, with contact between the ends of adjacent spines (1). Changed from 0 to ?.

Char. 112. Ossified tendons in distal region of tail: absent (0), present (1). Changed from 0 to ?.

Char. 113. Dimensions of coracoid: longer than wide (0), wider than long or equal width and length (1). Changed from 1 to 0.

Char. 116. Size of coracoid glenoid relative to scapula glenoid: sub-equal (0), half the size (1). Changed from ? to 0.

Char. 119. Ventral process of scapula at the caudoventral margin of glenoid: absent (0), present (1). Changed from 0 to 1.

Char. 121. Orientation of the acromion process of scapula: directed away from the glenoid (0), directed towards scapula glenoid (1). Changed from 0 to 1.

Char. 123. Distal end of scapula shaft: narrow (0), expanded (1). Changed from 1 to 0.

Char. 126. Angle of lateral deflection of the preacetabular process of the ilium: 10º–20º (0), 45º (1). Changed from 1 to ?.

Char. 127. Orientation of the preacetabular portion of the ilium: near vertical (0), near horizontal (1). Changed from 1 to ?.

Char. 128. Form of the preacetabular portion of the ilium: straight process (0), pronounced ventral curvature (1). Changed from 1 to ?.

Char. 138. Ratio of deltopectoral crest length to humeral length: $\leqslant$ 0.5 (0), > 0.5 (1). Changed from 0 to ?.

Char. 150. Maximum distal width of the tibia, compared to the maximum proximal width: narrower (0), wider (1). Changed from 0 to ?.

Char. 151. Contact between tibia and astragalus: articulated (0), fused, with suture obliterated (1). Changed from 0 to ?.

Char. 155. Dimensions of largest osteoderm: no osteoderms (0) smaller than a dorsal centrum (1), equal to or larger than a dorsal centrum (2). Changed from 1 to 0.

Char. 170. Lateralmost osteoderms in thoracic region: absent (0), ovoid or sub-ovoid with a longitudinal keel (1) triangular, dorsoventrally flattened elements (2), solid, conical spikes (3). Changed from 2 to 3.

Char. 173. Caudal osteoderms: absent (0), present on dorsal or dorsolateral surfaces of tail only (1), completely surrounding tail (2). Changed from 1 to ?.

Char. 174. Morphology of proximal, lateral caudal osteoderms: osteoderms absent (0), triangular with round/blunt apex (1) triangular with pointed apex (2). Changed from 2 to ?.

Char. 176. Tail club knob shape: knob absent (0), major knob osteoderms semicircular in dorsal view (1), triangular in dorsal view (2). Changed from 0 to ?.

Char. 189. Shape and texture of millimeter-sized ossicles: amorphous or polygonal ossicles with irregular texture (0), oblate spheroid to squared ossicles with conspicuous orthogonal fibers on the inner surface (1). Changed from 0 to ?.

Patagopelta cristata (previously as "Argentinean nodosaurid" or "Salitral Moreno ankylosaur").

Char. 90 Maxillary and/or dentary tooth denticles: < 13 denticles (0), $\geqslant$ 13 denticles (1). Changed from ? to 0.

Char 97. Ratio of anteroposterior dorsal centrum length to posterior centrum height: > 1.1 (0), < 1.1 (1). Changed from 0 to 0 and 1.

Char 103. Longitudinal groove in ventral surface of the sacrum: absent (0), present (1). Changed from ? to 0 and 1.

Char. 105. Ratio of maximum distal width to height of the neural spines of proximal caudals: $\leqslant$ 0.2 (0), > 0.2 (1). Changed from 1 to 0.

Char. 156. Basal surface of osteoderms: no osteoderms (0) flat or gently concave (1), deeply excavated (2), strongly convex (3). Changed from 2 to [1 2].

Char. 171. Thoracic osteoderms coossified to dorsal ribs: no osteoderms coossified to ribs (0), at least some osteoderms coossified to ribs (1). Changed from ? to 0.

Antarctopelta oliveroi

Char. 108. Attachment of haemal arches to their respective centra: articulated (0), fused (1). Changed from ? to 0.

Char. 119. Ventral process of scapula at the caudoventral margin of glenoid: absent (0), present (1). Changed from ? to 1.

Char. 122. Scapulocoracoid buttress: absent (0), present (1). Changed from ? to 0.

Char. 154. Postcranial osteoderm distribution: no postcranial osteoderms (0); postcranial osteoderms arranged in multiple transverse rows (1); postcranial osteoderms primarily present in two rows along midline (2). Changed from ? to 1.

Char. 158. Haversian bone in osteoderms: no osteoderms (0) absent in core of skeletally mature osteoderms (1), may be present in in core of skeletally mature osteoderms (2). Changed from ? to 1.

Matrix S1 Matrix (191×67) for phylogenetic analysis of *Antarctopelta oliveroi*. The matrix is also provided in. tnt format at https://aps.chinare.org.cn/EN/10.12429/j.advps.2023.0036

Lesothosaurus diagnosticus

000000???0000000???00000000000000000000000000000000000000?000000000000000?0000001?00000000000000
000000?0?000000000000000000?0000?00000000000000100?00001000000000000000000000000000100?000??00

Scelidosaurus harrisonii

000000???0?00000???00000000010?000000110001100000000000000?1000000000??100100001?1100?0010000001011
0000??00?00000000?0000000?0010?00000011000??0000000001011[1 2]11110????110010121200000000000000000

Huayangosaurus taibaii

000000000000000000?00000000010??0000?11000100000000000000??11100000000010010?000111?00001001???1111
1?010001100000?0001000000?10100000000010?0???201010002122 1?????00000000001101000000 10?01?0?00

Paranthodon africanus

??????1??01???0??0?????????10?0??11100????????????????
??111??????????

Stegosaurus stenops

0000001000100000000?000000000100?0000?000001000000000000000??1110000000001001 0?000111?0001110????1111
1?010001100000?0001000000?10100000000010?0???201010002122 1?????0000000000110100111 01[0 1]10111??0

Ahshislepelta minor

??
???001111?110?????????????0001???????????????22121???????1??????????????????0??0??

Akainacephalus johnsoni

11110100?12100010??22212000111 1?11120211?1110?212010?10110101100001??11111000?11110?110???????1?0011
11100011110?0?1?00110?1?11111100?00??100???1011010????23??1?0231???1110??12221???31000???10

Aletopelta coombsi

??111??????????????0???0
?0????????????????1??????0?????????????1111??1?2???????2????1???3?1????001????0?????

Animantarx ramaljonesi

101?1?????????????????????????????11??11?0011??0?0001101?111???????10110??1111110????1?0????111111?1??
???????10011112101?1111?01111011011??????110?????????????????????????????0?1????0????1

Ankylosaurus magniventris

11110100?11?112101?231010111101110 11?210?11101212010211111111110000111111111101111001?211111???1111111
??000011311???01110010????0?????0110100???2010111???122?????22100??????1??121000??000???00

Anodontosaurus lambei

11110100?11111110?1231010111111110111210111101212110211111111110000111111111101111001?21111?????????11
10?00?11111????????????1110011?101001??????01011112?122??????220??????????23100131?00?0???

Borealopelta markmitchelli

1?100000???0??01???22101102?1????011?2100??1012120010?????????????????????????1??????1111??????????1????
???????????????1??????????????????????01??????????122?????3101101130??????1?????????????

Cedarpelta bilbeyhallorum

11100?00?01?0?0????10000?00?100?1000?1?0??1?0????000??101?11110??0???01?1111011??1????00??????1??????1
100??0?0???11???????????????????011010????10101??????????????????????????????????320?0????1?

Chuanqilong chaoyangensis

1??1???101?111?????????????????1111?0???111????1??101???????
000?1????0100001?11100011?0000100??2211?11102??2?????0?????0????????001111???00?????

Crichtonpelta benxiensis
111101???????????1?1000000011????000?211011?0121101011110???11000?1?011111???????????????????110111110
010?0????00101111010?11100?1?1??0000????20101110??????????????????????????1???211?0????0
Denversaurus schlessmani
10101?0??120??00???2110100??1????0???11???1?001110??0?????1?00????????111??????????????????????????????
???1011??????????
Dongyangopelta yangyanensis
??11110?????
???????????????????????????????????1??????????122???????????12??2???????????????????
Dyoplosaurus acutosquameus
??1????????????????2?10??????????????11?1???0?????1021???????????????????????????????????1??????????????0100
111?1?????????????110011?101????0??2201?11112112????????????1111??12211?1?13100??00??
Edmontonia rugosidens
10101000?12001000??2110100111110?0???111??1?0011100100????11?1?11???01111101?1111100?011110?111?01111
11??2?1??0??????????????????????1???????????????????121?????3102?????????????1011[3 4]1??0????1
Edmontonia longiceps
11101000?12001000??2110100111110?01??11???11001110010?11?11111110???11111????111100?011?1???????????1
1?????????????????????11111?1011???11????????1?????111??????10???????1?????101131??0????1
Euoplocephalus tutus
11110100111111110112310101111111101112111111012120102111111111100001111111111011111011211110??01111111
1000001111101101110010111100111101001001?12010111121122211202210?111???12?12110021000??000
Europelta carbonensis
?0101???????????????2110????11?0??0???110????011110010110111???01??????101?1???101???10?1100??01?0101111
002?100??0?0?1??????0??????1?00111?????1?1101011??122????????????11?03???00000141100?????
Gargoyleosaurus parkpinorum
101000000111000000?221011000101??001?210??1101211000001 2?0111100?010?010010101111110??000010101????
1???0?0???????????????????????????0??????????211001????122221??2100??10202?2???100121100?????
Gastonia burgei
10100101?11?11000??10000000011101000?110?11101211000001110011100001?0111010001????????1000?????????1
111010?0001?????11020?1?111000100101 00?0???201010????1222112 1?2?0?120202?2100100131000??00?
Gobisaurus domoculus
11100110?01101010??100000000101?1000?110?111012120100111?011110000??00110100?1????????1???????????11?
???????11???????????????????0????0?0000???1??????????????????????0?????????0010????10?????1?
Hoplitosaurus marshi
??
???1000110200????????????????10???210110?1??121??????????020??2?????????????0??????
Hungarosaurus tormai
?0????01?0?10000?????????????1?0???????????1?0??111?????0???101??0??????1?1????1101110??0?00?1??1111111111
0001000?00111012001?1?10??1010?11000??1211010????12???????10???11??0???00?00132?00????0
Hylaeosaurus armatus
???00?0[0
1]110????????????00100110101?????????????????????????????????121???2??????????3?????????????????????
Jinyunpelta sinensis
111000011111??011??1000???011????000?21?0??????1?0?????????????????????????????1????0101??????01??1?11???
???0?1?1??????1??1????100?1??0?00?1?101????1???????????????????1????1???111??????00??0??
Liaoningosaurus paradoxus
???0111??????????0??0???0
1010????0?0??00?111000110010000?102?00?111000??????????????????????????111???0000??0
Mymoorapelta maysi
??11010?010?1
0010????????????1011010?01?00010??1??????????122???????????122?2?2?00??????00??????
Niobrarasaurus coleii
1??????????????????1000?????1????0???1????????11??111????1?1???1111110
000??????1???????1110??101??00011??21110101111112??????????010??????00?11131?00?0???
Nodocephalosaurus kirtlandensis
111??????????????????2?21???1?1???1011?22????1012120?0??1??11????????????1?111???????????????????????????????

0??2222120????0???????????1???????0?????

Nodosaurus textilis

??111111???0
00?0????????????111??1101?????????1111?1?011?12????2??????000?0312???????31100?30??

Panoplosaurus mirus

10101100???0??000??21101101?1???101??110??1?0011100100?0101111111??0111101?1111?101211???0111????1?
11?????????1000110200 1????????????1101?1?1???????1??121????12100????????????1001?10?00??11

Paw Paw scuteling

??????????????????????????11?????????????????????????0?0?1?????????????11?????????????111???01?11?????????
0????000?0??21???1?100??????0000??????0?1??????????????????????????????1?1????0?????

Pawpawsaurus campbelli

10101000?02?00010??22211102110001011?110111101111001001100111111111011101101 01???????01?????????????
???0???????????1?0?????????0?

Peloroplites cedrimontanus

?0101?00?111???????2?10??????????????110?01?001110000110?0101?0???????11?1???0???000??1000???01?10011?1
012?0?????1??1112101?111000111????????0110111000??????????????????????????000?1?00????1

Pinacosaurus grangeri

111101001111 10101?01000200?1111011?20221011001211 01??1111111110000111011011101111100111111 0??01?1111
1100?0011111010011?10?0111100111101001001012010111121122????02210101020?1221210113??0000?00

Pinacosaurus mephistocephalus

11110100?????101???0?010???11???0?1?211?1100222101??1?0??????????????????????1?10???1111101????????11??
??011111????1111??0?11100????????10?10???????????122????022100???1???????1011?1?0??????

Polacanthus foxii

???1???211???????????????????????????????????0??????01??1?01?110101
000?1100?11??????1010001011????????121101011??122100???101?0202021??00????4100???0??

Saichania chulsanensis

1111000111111111??2222110111011101112110111012121101111111111110001110111111111111011211110111111??11
????????????1??1?110?01???????????10100101??????????122????0222000??10??????111131100?0?0?

Sauropelta edwardsorum

101010????????????????0??????0??10???1100111011110 1?0001101111 1??11??1001?101111110?1?1101110?0110101
1110000010100011121010111010101101001110211101001111 22????13201?0113011110011013?100000?0

Sauroplites scutiger

???1?????????
???1?2???????????12???2????????????????????

Scolosaurus cutleri

11110?????????1??1?23101?1111????011?211??1101212110211111111110???????111111???????????111???????1???100
?0011111011?1110??0?1110011010?001????1????11?121122?????2210111110112212101131??0??0?0

Shamosaurus scutatus

11100110?011?1010??100000000101?1000?110?111012120101110101111100 11?0011011??1111000?11??????????????
???1???????2210????????????1?????????????0

Silvisaurus condrayi

10101000?02000000??21101???0100?10???110?11?0011100?000110111111?11?0110110101 1111????01111???1111110
10?1??0???????????????0??????????????????????????????122?????3101????????????1111?1??????0?

Stegopelta landerensis

??1?????00?1?1?????????
???????????20?1????????????????1??????????????????????10??????13??????001??????????

Struthiosaurus austriacus

?01?1???????????????2?10???????????????11?????0?????01100?0?1???????????11110?0?111????0?1??????0?10?111?1?
??1????????11020?0?11100?1??0????????1211010????121?????3101??00?????????000??100????0

Struthiosaurus languedocensis

???111??????10111111???1
000?????????????111?1?1000??????????????????121???????????10?????????00041?0??????

Struthiosaurus transylvanicus

?01?0???????????????2?1?????????????????1????0?????0101????????1???????1111??????????????????000????1??????
??????????11120?0??

Talarurus plicatospineus

111100??????????102?21??0???????0?1?210?1?1012??01021?1??????0???????111110?????????????????11?011100
0001111101101111000?111001111010010010120101111??12???????2?0?????0??????1??????0????00

Taohelong jinchengensis

???1????10??
????????????????1?1?1?10?????????????????????12?????????????12???2???????????????????

Tarchia kielanae

11110001111?1?111??222212021111?1122?221?11012222110101010111110000?010111111111111011211110?????????
??0?

Tatankacephalus cooneyorum

?0101???????1??????2110????0111??????11??1?101111?0?00?1??????1?01?1?0?010010?????????0111??????????????
???2?????????????????????1100????????0?

Texasetes pleurohalio

??111????1???????1????0
????1001111210??????????????0?111???1101??01???????????????????????????001??110?????

Tsagantegia longicranialis

11100000?11111000??22101001111101011?210?1110121?01011111111111110001?001111?10?????????11??0???????????
???1?????????????

Zaraapelta nomadis

111?00?????????????02?22???2?1???1?221220?1110121211000111111111001?1??1111110??????????????????????????
???

Zhejiangosaurus lishuiensis

??1???1101?001
????????????????11100?111?1???????1211011?12??????????????????????????????????11??????

Ziapelta sanjuanensis

1111010??11??1110??231010111111??011?211?11101???01021??????1?0?0?1???1111??0?????????1?????????????????
???1?2??????220?????????????1????????????0?

Zuul crurivastator

11110100?110?1110??231010111111?1012?2111111012121102111111111100001?00111111?1111000?001000??0???1?1?
?0?0?011111?????????????1??0011???????????????????????122????1?????1112??122111100???0???00?

Patagopelta cristata

???11???????????????????????????????????????1?0??????[0 1]11???[0 1]
00210???????????????????????????????????????111110???12[1 2]2124??101??11?0??11???011??????????

Kunbarrasaurus ieversi

111000????????0????2???????110??10???210??1??????00???001111110???1??01001010?1?11????11?0??01??????10?
????0??1????0???????0010???0?00?000??????????????12[1 2]????111002111104212??0011??121??11?

Stegouros elengassen

??????01???0??00????0??????11????????11??????????????00????????????0????100001???011??00?1000??01001110100
021000??101?0??????011101001?10??010101011010000012[1 2]?????????2111?0421200001110121101??

Antarctopelta oliveroi

???1??????100????1????1?100?21
0???1???0011??0??????????????????????????????????1?[1 2]21?4??????111?042?2???011?012???1??

Minmi paravertebra

??0[0
1]1?11???1????????????????????????1??????????????????????1??

SAMA_P40536

??????????????????????????1??0??100??????????????????
???011?????????1?